

## THE CRYSTAL CHEMISTRY OF THE SILICATE GARNETS

G. A. NOVAK<sup>1</sup> AND G. V. GIBBS, *Department of Geological Sciences,  
Virginia Polytechnic Institute and State University,  
Blacksburg, Virginia 24061*

## ABSTRACT

Refined structures of eight natural garnets [Cr-pyrope, almandine, spessartine, Mn-grossular, grossular, uvarovite, goldmanite, and andradite] are compared with that of synthetic pyrope to determine the effects of the substituent cations on polyhedral interactions, bond lengths, and angles. The Si-O bonds in these garnets constitute two populations which can be related to  $\langle r\{X\} \rangle$ , the mean radius of the  $X$  dodecahedral cation. If  $\langle r\{X\} \rangle$  is less than 1.0 Å, then Si-O =  $1.635 \pm 0.005$  Å, but if  $\langle r\{X\} \rangle$  exceeds 1.0 Å, then Si-O =  $1.650 \pm 0.005$  Å. However, the X-O and Y-O bond lengths and the O-X-O, O-Y-O, and O-Si-O angles are linearly dependent on  $\langle r\{X\} \rangle$  and on  $\langle r\{Y\} \rangle$  (where  $\langle r\{Y\} \rangle$  = the mean radius of the  $Y$  octahedral cation). A multiple linear regression analysis indicates the positional parameters of these garnets to be related to  $\langle r\{X\} \rangle$  and  $\langle r\{Y\} \rangle$  using Shannon and Prewitt's effective radii as follows:

$$x = 0.006 + 0.022\langle r\{X\} \rangle + 0.014\langle r\{Y\} \rangle$$

$$y = 0.051 - 0.023\langle r\{X\} \rangle + 0.037\langle r\{Y\} \rangle$$

$$z = 0.643 - 0.009\langle r\{X\} \rangle + 0.034\langle r\{Y\} \rangle.$$

The positional parameters of Fe-pyrope calculated with these equations [ $x=0.0336$ ;  $y=0.0491$ ;  $z=0.6530$ ] are in statistical agreement with the observed [ $x=0.0339(5)$ ;  $y=0.0491(6)$ ;  $z=0.6535(6)$ ] (Euler and Bruce, 1965). Furthermore, using a cell edge calculated from an equation obtained by regression analysis of 56 well characterized silicate garnets [ $a=9.04+1.61\langle r\{X\} \rangle+1.89\langle r\{Y\} \rangle$ ], the predicted positional parameters give bond lengths and angles that are statistically identical with those observed.

These equations were used to predict the structural details of over 200 hypothetical cubic silicate garnet compounds by assigning  $\langle r\{X\} \rangle$  values between 0.80 and 1.50 Å and  $\langle r\{Y\} \rangle$  values between 0.50 and 1.15 Å (at 0.05 Å intervals). Using criteria based on reasonable O-O, Si-O, X-O, and Y-O distances, a diagram was prepared in which the structural "stability" field of silicate garnets is delineated as a function of  $\langle r\{X\} \rangle$  and  $\langle r\{Y\} \rangle$ .

## INTRODUCTION

The garnet minerals comprise an important and widespread group of rock-forming silicates distinguished by their chemical diversity, close structural similarity, physical properties, and petrogenetic implications. They are cubic (space group  $Ia3d$ ;  $a=11.5-12.5$  Å), possess a relatively high refractive index ( $n=1.70-1.94$ ) and density ( $\rho=3.5-4.3$ g/cc), are hard ( $M=6.5-7.5$ ), and when rare-earth varieties are included, can exhibit any color of the visible spectrum. In solid-state technology, garnet has received attention because of the discovery of ferrimagnetism in

<sup>1</sup> Now at the Dept. of Geology, California State College at Los Angeles, Los Angeles, California, 90032.

$\{Y_3\}[Fe_2 \uparrow \uparrow](Fe_3 \downarrow \downarrow \downarrow)O_{12}$  and antiferromagnetism in  $\{Ca_3\}[Fe_2 \uparrow \downarrow](Si_3)O_{12}$  (Bertaut and Forrat, 1956; and Geller and Gilleo, 1957). A few rare-earth garnets have also been found to possess good laser properties (Geusic *et al.*, 1964).

Some garnets are slightly birefringent (*cf.* Yoder, 1950; Dillon, 1958) and others can be spontaneously polarized in electric and magnetic fields and accordingly cannot be cubic (Geller, 1967). The resolving power of X-rays has not, as of yet, detected this noncubicity for a silicate garnet although Prewitt and Sleight (1969) have found  $\{Cd_3\}[Cd Ge](Ge_3)O_{12}$  to be tetragonal and to have a derivative structure of garnet.

The general chemical structural formula for an oxide garnet, with eight formula units per cell, can be written:  $\{X_3\}[Y_2](Z_3)O_{12}$ . The notation in the formula (Geller, 1967) designates the type of oxygen coordination polyhedra formed about each X, Y, and Z cation: { } refers to an 8-fold triangular dodecahedral coordination, [ ] refers to a 6-fold octahedral coordination, and ( ) refers to a 4-fold tetrahedral coordination. The various cations known to occupy these three positions are enumerated for all garnets by Geller (1967), and for the silicate garnets ( $Z$ ) = Si, by Rickwood (1968). Winchell (1933) has divided the silicate garnets into two groups: (1) the *ugrandites*,  $\{X\} = Ca$ , made up of end-members uvarovite  $\{Ca_3\}[Cr_2](Si_3)O_{12}$ , grossular  $\{Ca_3\}[Al_2](Si_3)O_{12}$ , and andradite  $\{Ca_3\}[Fe_2](Si_3)O_{12}$ , and intermediate compositions; and (2) the *pyralspites*,  $\{X\} \neq Ca$ , with end-members pyrope  $\{Mg_3\}[Al_3](Si_3)O_{12}$ , almandine  $\{Fe_3\}[Al_2](Si_3)O_{12}$ , spessartine  $\{Mn_3\}[Al_2](Si_3)O_{12}$ , and also all intermediate compounds. Garnets of end-member composition are rare. Other rock-forming garnets pertinent to this study are goldmanite  $\{Ca_3\}[V_2](Si_3)O_{12}$  and knorringite (= hanléite)  $\{Mg_3\}[Cr_2](Si_3)O_{12}$ .

Menzer (1926) first solved the structure of grossular using powder methods, and later (1929) established that the remaining *ugrandites* and *pyralspites* are isostructural with grossular. He found that the  $\{X\}$ ,  $[Y]$ , and  $(Si)$  cations are in special positions with site symmetry  $D_2$ ,  $S_6$ , and  $S_4$ , respectively, and that oxygen is in a general position with  $x \approx 0.04$ ,  $y \approx 0.05$ , and  $z \approx 0.65$ . Descriptions of the garnet structure are numerous (*cf.* Abrahams and Geller, 1957; Zemann, 1962; Gibbs and Smith, 1965; Prandl, 1966; Geller, 1967). Briefly, it consists of alternating  $SiO_4$  tetrahedra and  $YO_6$  octahedra, which share corners to form a continuous three dimensional framework (Figure 1). The oxygen atoms in the framework also define triangular dodecahedra consisting of eight oxygens which coordinate the X-cations, each of these oxygens being coordinated by one (Si), one  $[Y]$  and two  $\{X\}$  cations. This results in a high percentage of shared edges (see Table 1), which may explain the relatively high density and refractive index of garnet (Gibbs and Smith, 1965).

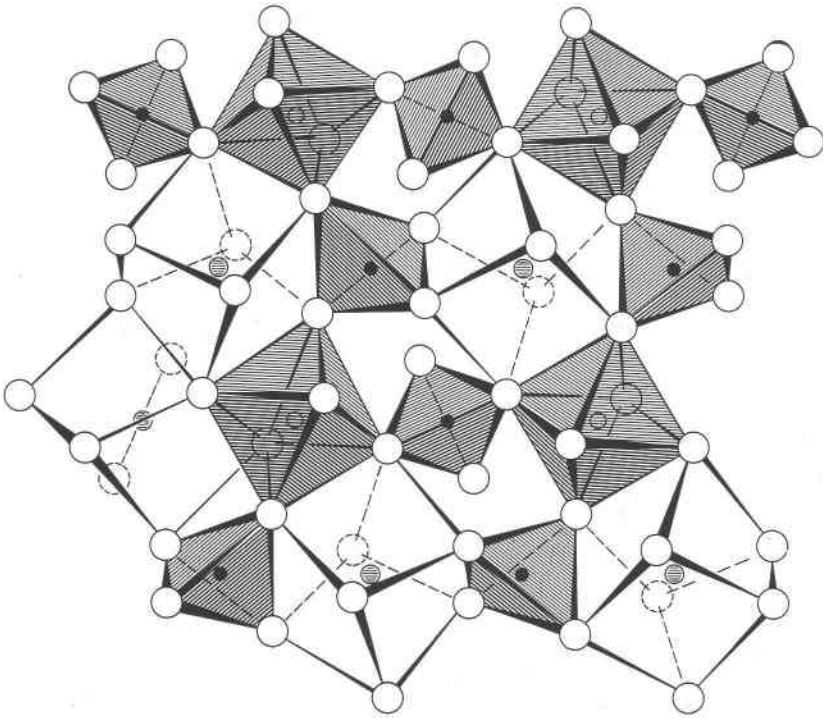


FIG. 1. Portion of the garnet structure projected down  $z$  showing the framework of alternating tetrahedra and octahedra (shaded portion) and the 8-fold triangular dodecahedra coordinating the  $\{X\}$  cations. The triangular dodecahedra are drawn as distorted cubes. Large open circles represent oxygens, smaller ones the  $\{Y\}$  cations, solid circles the  $\{Si\}$  cations, and the hatched ones the  $\{X\}$  cations.

Although Menzer solved the garnet structure over 40 years ago, only four silicate garnets, namely, natural grossular (Abrahams and Geller, 1957; Prandl, 1966), synthetic pyrope (Zemann and Zemann, 1961; Gibbs and Smith, 1965), a natural Fe-pyrope (Euler and Bruce, 1965), and a

TABLE 1. THE NUMBER AND TYPE OF SHARED POLYHEDRAL EDGES  
IN THE GARNET STRUCTURE

Polyhedron	Shared Edges
Tetrahedron	2 with triangular dodecahedra
Octahedron	6 with triangular dodecahedra
Triangular dodecahedron	2 with tetrahedra 4 with octahedra 4 with other triangular dodecahedra

natural andradite (Quarene and de Piere, 1966), have since been refined by modern methods. Selected results of these refinements are given in Table 2 including experimental methods, Si-O bond lengths, and the shared and unshared edge lengths of the  $YO_6$  octahedron. A detailed discussion of the structures of several of these garnets is given by Geller (1967) in a comprehensive review of the general crystal chemistry of garnets. The different types of experimental methods of data collection and application of weighting schemes, and the relatively large estimated standard errors (e.s.d.'s) in certain cases, make meaningful comparisons of the bond lengths difficult. Geller (1967) does, however, infer from these data that Si-O distances are less affected by a change in the size of the  $\{X\}$  cation than are Al-O distances. An important structural anomaly noted in Table 2 is that the octahedral edge shared with the triangular dodecahedron in grossular is longer than the octahedron's unshared edge,

TABLE 2. SUMMARY OF SILICATE GARNET SINGLE CRYSTAL STRUCTURE REFINEMENTS COMPLETED PRIOR TO THE PRESENT STUDY

Garnet	Method of Data Collection	Weighting Scheme	Si-O (Å)	O-O Octahedral Edge Shared	O-O Octahedral Edge Unshared
Grossular <sup>a</sup>	Weissenberg multiple film methods	Based on the relative intensities and the multiplicity of each observed reflection.	1.64 (2) <sup>g</sup>	2.79 (6)	2.71 (6)
Pyrope <sup>b</sup>	Integrating Weissenberg multiple film methods.	Unit weights, $w=1.0$	1.62 (2)	2.64 (2)	2.72 (2)
Pyrope <sup>c</sup>	Scintillation-counter equi-inclination Weissenberg diffractometer.	Unit weights, $w=1.0$	1.635 (2)	2.618 (3)	2.716 (3)
Grossular <sup>d</sup>	Precession film methods.	$w=1/\hat{\sigma}^2$ , where $\hat{\sigma} = (\sum_j (Fo_j - \langle Fo \rangle)^2 / n(n-1))^{1/2}$ .	1.651 (2)	2.755 (3)	2.695 (3)
Fe-Pyrope <sup>e</sup>	Weissenberg counter diffractometer as in pyrope.	$w=1/\epsilon^2$ , with $\epsilon=1/s$ where $s$ is the scale factor.	1.635 (7)	2.658 (11)	2.724 (13)
Andradite <sup>f</sup>	Weissenberg multiple film methods.	Based on a modification of Cruickshank's (1965) weighting scheme.	1.66 (1)	2.84 (2)	2.79 (2)

<sup>a</sup> Abrahams and Geller (1957).

<sup>b</sup> Zemann and Zemann (1961).

<sup>c</sup> Gibbs and Smith (1965).

<sup>d</sup> Prandl (1966).

<sup>e</sup> Euler and Bruce (1965).

<sup>f</sup> Quarene and de Piere (1966).

<sup>g</sup> The numbers in parentheses are the e.s.d.'s and refer to the last significant number.

in violation of Pauling's (1929) rules. Since this is not true for pyrope, the greater length of the shared edge in grossular may be attributed to presence of Ca rather than Mg in the {X} site.

A great deal of work has been undertaken in the past two decades on the phase relations and occurrences of the silicate garnets (*cf.* Yoder, 1950; Yoder and Keith, 1951; Coes, 1955; Geller and Miller, 1959 a, b, c; Gentile and Roy, 1960; Geller, Miller, and Treuting, 1960; Zemann, 1962; Chinner and Schairer, 1962; Mill, 1964, 1966; Strens, 1965; Němec, 1967; Geller, 1967; Hsu, 1968; Ito and Frondel, 1968; and Hsu and Burnham, 1969). These studies indicate that complete miscibility exists between all the geologically important garnets, even if only under very special conditions. Furthermore, they emphasize the importance of the relative sizes of the substituent cations in explaining miscibility as well as site preference and garnet stability. For example, Zemann (1962) suggests that {Fe<sup>2+</sup>} and {Mn<sup>2+</sup>} can be more easily accommodated into the [Al<sub>2</sub>](Si<sub>3</sub>)O<sub>12</sub> framework of garnet than the slightly too small {Mg<sup>2+</sup>} and the slightly too large {Ca<sup>2+</sup>}. He also argues that the framework cannot be stretched any further beyond that of grossular which has Ca<sup>2+</sup> in the {X} site.

Born and Zemann (1964) have since published on interatomic distances and lattice energies for these garnets. They found that the orientation and distorted nature of the SiO<sub>4</sub> tetrahedron (Zemann, 1962) could not be adequately explained in terms of attractive Coulombic forces alone but that it was also necessary to include repulsive forces of the type  $\lambda/d^n$  between adjacent oxygen anions and the {X<sup>2+</sup>} cations. Assuming the Si-O bond to be partially covalent with effective charges of +2.0 and -1.5 on Si and O, respectively, they obtained good agreement between the maximum of the partial lattice energy and the observed orientation of the tetrahedron; only moderate agreement was obtained when a fully ionic model was employed. Furthermore, from a consideration of the deformation and position angles of the tetrahedron (*cf.* their Fig. 2), they predicted that the unshared edges of the AlO<sub>6</sub> octahedron would be abnormally short when  $r\{X^{2+}\} > r\{Ca^{2+}\}$  whereas the unshared edge of the dodecahedron would be abnormally short when  $r\{X\} < r\{Mg^{2+}\}$ . These results lead them to suggest that silicate garnets with {X} cations larger than {Ca<sup>2+</sup>} or smaller than {Mg<sup>2+</sup>} are notably unstable.

The present study (Novak, 1970) was undertaken to expand our knowledge of the crystal chemistry of the silicate garnets. Structure refinements are presented for pyrope, Cr-pyrope, almandine, spessartine, Mn-grossular, grossular, uvarovite, goldmanite, and andradite using data determined from experimental procedures as identical as possible. Structural variations are enumerated in terms of the substituent cations

and various predictions about the structures are considered. Furthermore, the positional parameters of oxygen are related to the effective radii of the  $\{X\}$  and  $\{Y\}$  cations; a new equation is developed for the cell edge in terms of the chemistry of a silicate garnet and the structures of a number of possible silicate garnets are predicted solely from their composition. Garnet stability is then discussed in terms of the features of these predicted structures.

## EXPERIMENTAL

*Chemistry and Cell Dimensions.* The silicate garnets studied are named and coded in accordance with their dominant end-member molecule (Table 3). Chemical formulae, except those of the garnets enumerated below, were obtained from data collected with an ARL-EMX electron microprobe analyzer, using standard probe techniques (*cf.* Smith, 1965). Raw intensity data were reduced with the Rucklidge and Gasparrine (1968) EMPADR V program. Elemental proportions were first normalized to 12 oxygen atoms per formula unit, and then the relative cation proportions were adjusted assuming perfect stoichiometry. The chemical formula for goldmanite was taken from Moench and Meyrowitz (1964); Cr-pyrope from Novak and Meyer (*in press*); and that of pyrope from Gibbs and Smith (1965). The localities and sources of these garnets are given in Table 3.

Single crystals for X-ray examination were chosen for optical clarity, homogeneity, freedom from inclusions, size, and shape. They are nearly equidimensional and have diam-

TABLE 3. CHEMICAL FORMULAE, LOCALITIES AND SOURCES OF GARNET CRYSTALS

Garnet (Code)	$\{X_3\}[Y_2](Si_3)O_{12}$	Locality and Source
Pyrope (Py)	$\{Mg_{3.00}\}[Al_{2.00}](Si_3)O_{12}$	Synthesized by F. R. Boyd, Geophysical Laboratory, Washington, D.C.
Cr-Pyrope (Cr-Py)	$\{Mg_{2.68}Fe_{0.27}Ca_{0.09}Mn_{0.01}\}$ $[Al_{1.34}Cr_{0.57}Fe_{0.09}](Si_3)O_{12}$	Inclusion in a Venezuelan diamond supplied by H. Meyer, Goddard Space Flight Center, Greenbelt, Maryland.
Almandine (Al)	$\{Fe_{2.59}Mg_{0.27}Ca_{0.13}Mn_{0.01}\}$ $[Al_{1.98}](Si_3)O_{12}$	Emerald Creek in Latah Co., Idaho. U.S.N.M. #107105.
Spessartine (Sp)	$\{Mn_{2.58}Fe_{0.34}Ca_{0.08}\}$ $[Al_{1.99}Fe_{0.01}](Si_3)O_{12}$	Minas Gerais, Brazil. U.S.N.M. #107286.
Mn-Grossular (Mn-Gr)	$\{Ca_{1.34}Mn_{0.81}Fe_{0.76}Mg_{0.09}\}$ $[Al_{1.99}Ti_{0.01}](Si_3)O_{12}$	Locality unknown. VPI Mineral Collection.
Grossular (Gr)	$\{Ca_{2.96}Mn_{0.04}\}[Al_{1.95}Fe_{0.05}](Si_3)O_{12}$	Asbestos, Quebec supplied by R. Newton, University of Chicago.
Uvarovite (Uv)	$\{Ca_{2.99}Mn_{0.01}\}$ $[Cr_{1.73}Al_{0.21}Fe_{0.05}Ti_{0.01}](Si_3)O_{12}$	Washington, Nevada Co., Calif. VPI Mineral Collection.
Goldmanite (Go)	$\{Ca_{2.99}Mg_{0.08}Mn_{0.02}\}[V_{1.20}Al_{0.47}Fe_{0.33}](Si_3)O_{12}$	Laguna Uranium mining district, N.M. supplied by R. Moench, U.S.G.S., Denver, Colorado.
Andradite (An)	$\{Ca_{2.97}Mg_{0.02}Mn_{0.01}\}[Fe_{1.99}Al_{0.01}](Si_3)O_{12}$	Valmalen, Italy. U.S.N.M. #116725.

TABLE 4. MEASURED AND CALCULATED CELL EDGES ( $\text{\AA}$ ), MEASURED CELL VOLUMES  $V(\text{\AA}^3)$ , CALCULATED DENSITY (g/cc), MEAN RADIUS OF THE X-CATION ( $\langle r\{X\} \rangle$ ), MEAN RADIUS OF THE Y-CATION ( $\langle r\{Y\} \rangle$ ), MEAN CATION RADIUS ( $\langle r \rangle$ ), AND THE CUBED MEAN CATION RADIUS ( $\langle r \rangle^3$ ) OF NINE SILICATE GARNETS

Garnet	$a(\text{obs})$	$a(\text{calc})^b$	$a(\text{calc})^c$	$V(\text{obs})$	$\rho(\text{calc})$	$\langle r\{X\} \rangle$	$\langle r\{Y\} \rangle$	$\langle r \rangle$	$\langle r \rangle^3$
Py	11.459 (1) <sup>a</sup>	11.50	11.48	1504	3.53	0.890 $\text{\AA}$	0.530 $\text{\AA}$	0.746 $\text{\AA}$	0.415 $\text{\AA}^3$
Cr-Py	11.526 (1)	11.54	11.54	1531	3.96	0.898	0.559	0.760	0.439
Al	11.531 (1)	11.55	11.52	1533	4.29	0.919	0.531	0.762	0.433
Sp	11.612 (1)	11.62	11.61	1565	4.21	0.977	0.530	0.798	0.509
Mn-Gr	11.690 (1)	11.70	11.69	1597	3.94	1.022	0.531	0.826	0.563
Gr	11.845 (1)	11.85	11.84	1662	3.62	1.118	0.532	0.884	0.691
Uv	11.988 (1)	12.00	11.99	1723	3.82	1.119	0.610	0.915	0.766
Go	12.011 (1)	12.07	12.00	1732	3.75	1.114	0.615	0.914	0.763
An	12.058 (1)	12.04	12.06	1753	3.85	1.118	0.644	0.928	0.799

<sup>a</sup> Numbers in parentheses are the e.s.d.'s and apply to the last decimal place reported.

<sup>b</sup> Calculated from McConnell's (1966) equation.

<sup>c</sup> Calculated from the equation of this study.

eters in the range of 0.07–0.12 mm. Zero, first, and second level precession photographs were recorded for all crystals (except pyrope and Cr-pyrope) using Zr-filtered Mo-radiation. In all cases the most probable space group is  $Ia3d$ . Although the crystals of andradite and uvarovite examined are slightly birefringent, precession photographs exposed up to 200 hours display Laue and diffraction symmetry consistent with space group  $Ia3d$ . Cell edges were determined from high angle reflections of the type  $h00$  measured with a Picker single-crystal diffractometer.

As a check, cell edges were also calculated from the regression formula of McConnell (1966) using Ahrens' radii. The greatest discrepancies between observed and calculated cell edges (Table 4) are found for goldmanite and pyrope, where  $a(\text{calc})$  is about 0.05  $\text{\AA}$  greater than  $a(\text{obs})$ . Because McConnell's equation was obtained from few data and because the e.s.d.'s of his regression coefficients and intercept are relatively large, a multiple linear regression analysis was calculated for 56 chemically analyzed silicate garnets with well-determined cell edges. The new equation (multiple correlation coefficient,  $\hat{R}_1(a) = 0.996$ ) relates  $a$  to the mean radius of the X-cation,  $\langle r\{X\} \rangle$ , and the mean radius of the Y-cation,  $\langle r\{Y\} \rangle$ , using Shannon and Prewitt's (1969) effective radii as follows:

$$a = 9.04(2) + 1.61(4)\langle r\{X\} \rangle + 1.89(8)\langle r\{Y\} \rangle \quad (1)$$

where the numbers in parentheses are the e.s.d.'s of the intercept and regression coefficients and refer to the last significant figure quoted. Figure 2 is a plot of  $a(\text{obs})$  versus  $a(\text{calc})$  for the 56 garnets of the analysis. The largest difference between  $a(\text{obs})$  and  $a(\text{calc})$  is about 0.03  $\text{\AA}$ , with the mean difference less than 0.01  $\text{\AA}$ .

The radius of 8-coordinated  $\{\text{Fe}^{2+}\}$  is not given by Shannon and Prewitt; however, the values given for 4-coordinated ( $\text{Fe}^{2+}$ ) and 6-coordinated [ $\text{Fe}^{2+}$ ] were extrapolated to a value of 0.91  $\text{\AA}$  for 8-coordinated  $\{\text{Fe}^{2+}\}$ . Also, the value for  $\{\text{Mn}^{2+}\}$  of 0.93  $\text{\AA}$  given by Shannon and Prewitt resulted in predicted Mn-O distances approximately 0.05  $\text{\AA}$  less than those observed. A recent refinement of  $\{\text{Mn}_3\}[\text{Fe}_2](\text{Ge}_3)\text{O}_{12}$  by Lind and Geller (1969) yielded a mean Mn-O distance of 2.364  $\text{\AA}$ . Subtracting from this the radius of a 4-coordinated oxygen (1.38  $\text{\AA}$ ) gives an effective radius of 0.98  $\text{\AA}$  for  $\{\text{Mn}^{2+}\}$ , the value used here. Measured cell volumes, calculated densities,  $\langle r\{X\} \rangle$ ,  $\langle r\{Y\} \rangle$ , mean non-tetrahedral cation radius,  $\langle r \rangle = (24\langle r\{X\} \rangle + 16\langle r\{Y\} \rangle)/40$ , and the cubed mean cation radius,  $\langle r \rangle^3$ , are given in Table 4 for the nine silicate garnets of this study.

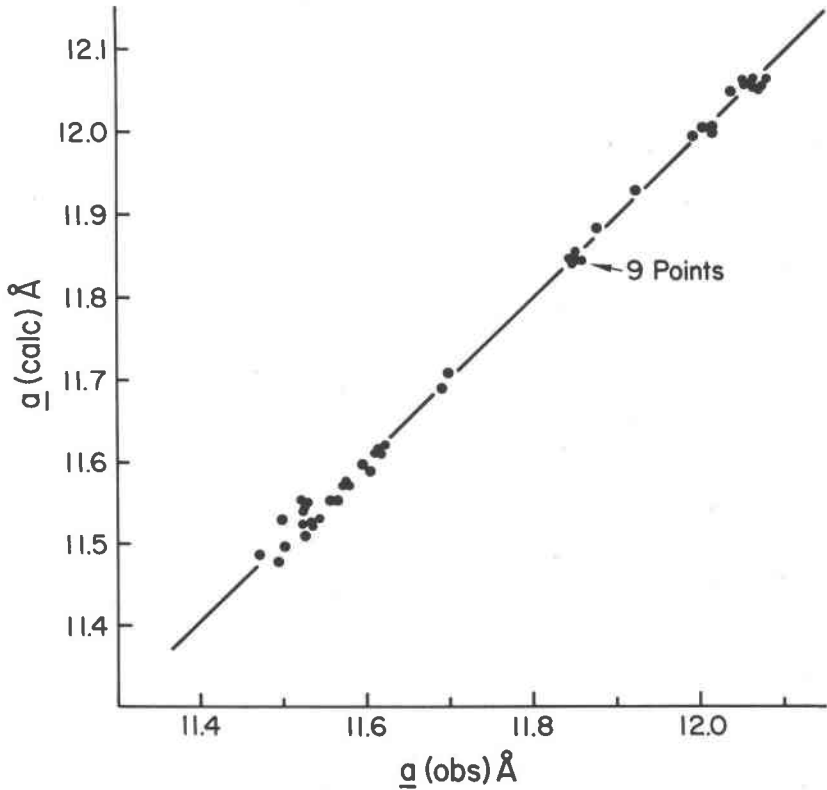


FIG. 2. Calculated cell edges  $a(\text{calc})$  plotted against observed cell edges  $a(\text{obs})$  for 56 silicate garnets, including 48 from other authors (Skinner, 1956; Abrahams and Geller, 1958; Geller and Miller, 1959c; Geller and Espenosa, unpublished data; Swanson *et al.*, 1960a; Swanson *et al.*, 1960b; Kohn and Eckart, 1962; McConnell, 1964; Geller *et al.*, 1964; Frondel and Ito, 1965; Strens, 1965; Prandl, 1966; Quarenì and de Piere, 1966; Hsu, 1968; Huckenholtz, 1969; and Moore *et al.*, 1969).

*Intensity Collection and Structure refinements.* Six- to eight hundred observable reflections, of which 150 to 200 are non-equivalent, were collected for seven of the nine garnets included in this study using a scintillation-counter, Nb-filtered  $\text{MoK}\alpha$  radiation, and equi-inclination Weissenberg techniques. Intensity data were not re-collected for pyrope or Cr-pyrope. The data were reduced using Lovell and Van den Hende's data reduction program; absorption corrections, being negligible, were not applied. Three dimensional least-squares refinements using Busing, Martin, and Levy's (1962) ORFLS program were carried out on all nine sets of data with neutral atom, relativistic scattering factors (Doyle and Turner, 1968) applied without correction for anomalous dispersion. Starting parameters for the non-Ca garnets were those of pyrope (Gibbs and Smith, 1965), and for the Ca-garnets, those of grossular (Prandl, 1966). Weights,  $w$ , were assigned to each observation following Hanson (1965), who proposed a weighting scheme that gives more weight to structural

amplitudes of intermediate magnitude, and less to the strong and weak ones, where systematic errors are greater. Hanson suggested that each amplitude,  $F_o$ , be weighted

$$w = 1.0 / (1.0 + ((F_o - PA \times F_T) / XX \times F_T)^2)^{\frac{1}{2}} \quad (2)$$

where  $PA$ ,  $F_T$ , and  $XX$  are adjustable parameters. These parameters are chosen to yield constant values of  $\langle w\Delta^2 \rangle$  in equally populated groups of increasing  $F_o$ , where  $\Delta = |F_o - sq F_c|$ , so that estimates of the standard errors allow for all random experimental errors, as well as for systematic errors in the model and in the experimental data (Cruickshank, 1965).

Each set of data was processed as follows: isotropic refinement with  $w = 1.0$ ; Hanson's weighting scheme was applied and  $F_o$ 's with large  $w\Delta$  were removed with  $PA$ ,  $F_T$ , and  $XX$  adjusted until essentially constant values of  $\langle w\Delta^2 \rangle$  in equally populated groups of increasing  $F_o$  were obtained. Finally, the resultant parameters were then used as starting parameters in a full anisotropic refinement with Hanson's weights. In order to test the assumption that all atoms exhibit apparent anisotropic thermal vibration, further refinements were carried out by varying the scale factor ( $sq$ ), the oxygen positional parameters, and the temperature factor coefficients  $\beta(ij)$  of only one atom, or in some cases, two. All refinements were then subjected to Hamilton's (1965)  $R$ -factor significance test to decide whether or not a refinement with, for example seventeen parameters (full anisotropic), is statistically more meaningful than one with seven parameters (anisotropic only on  $\{X\}$ ).

For all refinements, varying the anisotropic temperature factor coefficients produced statistically more significant results than varying the more constrained isotropic ones. However, the positional parameters calculated for pyrope are statistically identical to those obtained by Gibbs and Smith (1965). The more significant refinements of grossular and uvarovite are those in which the  $\beta(ij)$ 's of the  $\{X\}$  as well as the  $[Y]$  cations were varied; however, the positional parameters of grossular are identical with those obtained by Prandl (1966). For Cr-pyrope the  $\beta(ij)$ 's of all atoms had to be varied to produce the most significant refinement; its positional parameters are also identical with those published (Novak and Meyer, 1971).<sup>2</sup> Table 5 contains the number of observations (NO), the number of parameters varied (NV), the unweighted and weighted  $R$ -factors ( $R$  and  $wR$ ), and Hanson's weighting parameters ( $PA$ ,  $F_T$ , and  $XX$ ). The oxygen positional parameters from the most significant refinement are given in Table 6, as well as the isotropic temperature factor coefficients ( $B$ ) and r.m.s. equivalents. The anisotropic temperature factor coefficients ( $\beta(ij)$ ) from the full anisotropic refinements are given in Table 7. Orientations of the apparent vibration ellipsoids with respect to the crystallographic axis and the r.m.s. displacements were calculated with Busing, Martin, and Levy's (1964) ORFEE program and are given in Table 8. The orientations of the triaxial vibration ellipsoids of the  $\{X\}$  cations for all nine garnets conform to the distortions of the 8-coordinated cavities as Gibbs and Smith (1965) first found for pyrope. For the pyralspites and Cr-pyrope, the major axis of the vibration spheroid for the  $[Y]$  cations parallels the  $S_6$  axis, as previously found for pyrope by Gibbs and Smith (1965), whereas for the ugrandites and goldmanite it is normal to this axis as found by Prandl (1966) for grossular. The representation quadric characterizing the apparent vibration of the  $[Y]$  cation in Mn-grossular is statistically spherical. The representation quadrics of the  $(Si)$  cations for all nine garnets are also statistically spherical with indeterminate orientations. The apparent vibration triaxial ellipsoid of the oxygen atom in the nine garnets is statistically anisotropic, but no interpretation is offered.

<sup>2</sup> A listing of the observed and calculated structure amplitudes for the most significant refinements of all garnets (except for pyrope and Cr-pyrope) may be ordered as NAPS Document 01397 from National Auxiliary Publications Service of the A.S.I.S., c/o CCM Information Corporation, 909 Third Avenue, New York, New York 10022; remitting \$2.00 for microfiche or \$5.00 for photocopies, in advance, payable to CCMIC-NAPS.

TABLE 5. REFINEMENT PARAMETERS: NUMBER OF OBSERVATIONS (*NO*), NUMBER OF VARIABLES (*NV*), *R*-FACTORS (*R* AND *wR*), AND WEIGHTING ANALYSIS PARAMETERS (*PA*, *F<sub>T</sub>*, AND *XX*)

Garnet	<i>NO</i>	<i>NV</i>	<i>R</i> <sup>a</sup>	<i>wR</i> <sup>b</sup>	<i>PA</i>	<i>F<sub>T</sub></i>	<i>XX</i>
Py	262	7 { <i>X</i> } <sup>c</sup>	0.071	0.090	2.0	4.0	1.3
Cr-Py	513	17 <sup>d</sup>	0.038	0.046	7.0	6.0	2.3
Al	507	7 { <i>X</i> }	0.038	0.038	10.0	6.5	2.0
Sp	492	7 { <i>X</i> }	0.048	0.038	12.0	6.0	2.0
Mn-Gr	560	7 { <i>X</i> }	0.053	0.061	5.0	6.2	1.8
Gr	625	9 { <i>X</i> }, [ <i>Y</i> ]	0.036	0.046	2.2	5.8	4.0
Uv	739	9 { <i>X</i> }, [ <i>Y</i> ]	0.033	0.030	11.5	5.8	3.0
Go	509	7 { <i>X</i> }	0.043	0.046	4.0	9.0	1.8
An	557	7 { <i>X</i> }	0.037	0.034	15.0	3.0	3.5

<sup>a</sup> Unweighted *R*-factor, where  $R = \Sigma |F_o - sq F_c| / \Sigma |F_o|$ .

<sup>b</sup> Weighted *R*-factor, where  $wR = (\Sigma w(F_o - F_c)^2 / \Sigma w F_c^2)^{1/2}$ .

<sup>c</sup> Parameters that were varied (in this case cation temperature factor coefficients {*X*}) in addition to the scale factor and the oxygen positional parameters.

<sup>d</sup> Full anisotropic.

Interatomic distances and angles and their associated e.s.d.'s calculated from the parameters of the most significant refinement, are listed in Tables 9 through 12. The numbers associated with the designations of interatomic distances and angles correspond to the atom nomenclature of Figure 3. It is emphasized that all oxygen atoms are symmetrically equivalent as well as all {*X*}, all [*Y*], and all (Si) cations and that the nomenclature of Figure 3 is devised only for convenience of presentation. Table 9 contains the structural data of the SiO<sub>4</sub> tetrahedron and the YO<sub>6</sub> octahedron; Table 10 the XO<sub>3</sub> triangular dodecahedron; Table 11 metal-metal distances; and Table 12 the observed angles, *M-O-M*, about oxygen. Table 13 contains various polyhedral distortion parameters such as bond strains (unshared minus shared polyhedral edges) and bond angle strains (observed angle minus the ideal angle for a given polyhedron). A discussion of the structural data is presented in the following section.

## DISCUSSION

*Cell Volumes and Cation Radii.* Figure 4 is a plot of cell volumes versus  $\langle r \rangle^3$  for the {*X*} = Ca and [*Y*] = Al garnet series. Cr-pyrope is not included in this or later figures because it is not a member of either series. The observed break in slope at grossular (Gr) points to the existence of the two series enumerated above. The greater slope for the Ca garnets and the regression coefficients of equation (1), both indicate that the cell edge increases more rapidly with increasing  $\langle r[Y] \rangle$  than with increasing  $\langle r\{X\} \rangle$ . For spessartine (Sp), Mn-grossular (Mn-Gr) and almandine (Al) the proximity of the data to the line substantiates the choice of  $r\{Mn\}$  and  $r\{Fe\}$  proposed in the experimental section of this study.

TABLE 6. OXYGEN POSITIONAL PARAMETERS, ISOTROPIC TEMPERATURE FACTORS AND THE R.M.S. EQUIVALENTS OF O, {X}, [Y], AND (Si) ATOMS FOR NINE SILICATE GARNETS.

ATOM	P <sub>Y</sub>	Cr-P <sub>Y</sub>	Al	Sp	Mn-Gr	Gr	U <sub>v</sub>	Go	An
0									
x <sup>a</sup>	0.03285(13) <sup>b</sup>	0.03346(9)	0.03427(10)	0.03510(8)	0.03577(13)	0.03808(11)	0.03991(16)	0.03850(20)	0.03986(15)
Y	0.05015(12)	0.05070(10)	0.04860(11)	0.04766(11)	0.04633(13)	0.04493(11)	0.04737(15)	0.04742(20)	0.04885(13)
z	0.65335(12)	0.65366(9)	0.65332(11)	0.65261(10)	0.65177(12)	0.65140(9)	0.65354(17)	0.65387(18)	0.65555(15)
B <sup>c</sup>	0.502(21)	0.679(16)	0.352(15)	0.378(14)	0.754(22)	0.764(21)	0.461(19)	0.898(28)	0.577(21)
<μ> <sup>d</sup>	0.080(2) <sup>e</sup>	0.093(1)	0.067(1)	0.069(1)	0.098(1)	0.098(1)	0.076(2)	0.103(2)	0.084(2)
{X}									
B	0.789(29)	0.637(15)	0.489(12)	0.477(10)	0.801(13)	0.612(14)	0.385(25)	0.643(20)	0.383(9)
<μ>	0.100(2)	0.090(1)	0.079(1)	0.078(1)	0.101(1)	0.088(1)	0.069(2)	0.090(1)	0.069(1)
[Y]									
B	0.397(23)	0.303(7)	0.265(10)	0.430(13)	0.619(15)	0.664(19)	0.252(8)	0.428(9)	0.494(17)
<μ>	0.071(2)	0.020(2)	0.058(1)	0.074(1)	0.089(1)	0.091(1)	0.057(1)	0.074(1)	0.079(1)
(Si)									
B	0.194(20)	0.337(12)	0.194(15)	0.350(14)	0.535(15)	0.558(17)	0.253(24)	0.433(28)	0.477(25)
<μ>	0.050(3)	0.065(1)	0.050(2)	0.067(1)	0.082(1)	0.084(1)	0.057(4)	0.071(3)	0.077(2)

a. x, y, and z are the positional parameters from the statistically most significant refinement. b. The numbers in parentheses are the e.s.d.'s. c. Isotropic temperature factors. d. R.M.S. displacement. e. E.S.D.'s for the root-mean-square displacements <μ> were calculated using the expression  $\delta\langle\mu\rangle = \delta(B)/16\pi^2\langle\mu\rangle$ .

TABLE 7. ANISOTROPIC TEMPERATURE FACTOR COEFFICIENTS,  $\beta_{ij}$ .

ATOM	$i, j$ of $\beta_{ij}$	Py	Cr-Py	Al	Sp	Mn-Gr	Gr	Uv	Go	An
0	11	0.00104(7) <sup>a</sup>	0.00130(7)	0.00071(8)	0.00075(7)	0.00165(10)	0.00147(7)	0.00102(8)	0.00194(14)	0.00102(8)
	22	0.00103(7)	0.00142(6)	0.00062(6)	0.00088(6)	0.00149(8)	0.00145(8)	0.00076(7)	0.00109(10)	0.00115(8)
	33	0.00087(6)	0.00115(6)	0.00066(7)	0.00056(6)	0.00194(7)	0.00112(7)	0.00058(9)	0.00142(11)	0.00071(9)
	12	0.00012(5)	0.00006(5)	0.00009(5)	0.00013(6)	0.00003(6)	-0.00004(6)	0.00002(10)	0.00001(9)	0.000016(9)
	13	-0.00005(5)	-0.00019(5)	0.00005(6)	-0.00015(7)	0.00003(7)	0.00008(6)	-0.00018(8)	-0.00029(10)	-0.00018(8)
	23	-0.00005(5)	0.00003(6)	0.00008(6)	-0.00002(6)	-0.00016(6)	0.00002(7)	-0.00009(7)	0.00002(9)	0.00002(6)
{X} <sup>b</sup>	11	0.00121(9)	0.00096(5)	0.00074(4)	0.00071(3)	0.00121(3)	0.00089(4)	0.00049(4)	0.00095(7)	0.00069(7)
	22	0.00170(7)	0.00134(4)	0.00102(3)	0.00100(2)	0.00165(3)	0.00119(3)	0.00074(3)	0.00122(5)	0.00092(4)
	23	0.00039(7)	0.00033(5)	0.00005(4)	0.00014(3)	0.00009(5)	0.00010(3)	0.00015(10)	0.00014(9)	0.00005(7)
[Y] <sup>c</sup>	11	0.00075(4)	0.00059(1)	0.00052(2)	0.00076(2)	0.00112(3)	0.00116(3)	0.00046(1)	0.00075(1)	0.00067(2)
	12	0.00001(3)	-0.00003(3)	0.00009(3)	-0.00003(4)	-0.00002(6)	-0.00017(4)	-0.00018(6)	-0.00004(5)	-0.00006(4)
(Si) <sup>d</sup>	11	0.00039(5)	0.00068(4)	0.00040(6)	0.00068(5)	0.00118(5)	0.00111(6)	e	0.00076(10)	0.00069(11)
	33	0.00043(9)	0.00055(8)	0.00026(11)	0.00046(9)	0.0053(9)	0.00079(10)	e	0.00071(20)	0.00107(18)

a. Numbers in parentheses are the e.s.d.'s. b. Symmetry constraints require  $\beta(22) = \beta(33)$  and  $\beta(12) = \beta(13) = 0.0$ .  
 c.  $\beta(11) = \beta(22) = \beta(33)$ , and  $\beta(12) = \beta(13) = \beta(23)$ . d.  $\beta(11) = \beta(22)$  and  $\beta(12) = \beta(13) = \beta(23) = 0.0$ . e. Indeterminate.

TABLE 8. R.M.S. DISPLACEMENTS AND ORIENTATIONS OF THERMAL VIBRATION ELLIPSOIDS WITH RESPECT TO THE CRYSTALLOGRAPHIC AXES OF THE ATOMS<sup>a</sup> OF NINE SILICATE GARNETS.

GARNET	r <sup>b</sup>	OXYGEN ATOM			{X} CATION			{Y} CATION					
		u(r) <sup>c</sup>	$\theta(r,x)^\circ$	$\theta(r,y)^\circ$	$\theta(r,z)^\circ$	u(r) <sup>d</sup>	$\theta(r,x)^\circ$	$\theta(r,y)^\circ$	$\theta(r,z)^\circ$	u(r) <sup>e</sup>	$\theta(r,x)^\circ$	$\theta(r,y)^\circ$	$\theta(r,z)^\circ$
Py	1	0.075(3)	167(9)	100(33)	81(32)	0.090(3)	90	90	180				
	2	0.078(3)	89(44)	136(15)	134(14)	0.093(3)	45	45	90				c
	3	0.088(3)	103(8)	47(10)	135(11)	0.118(2)	135	45	90				
Cr-Py	1	0.083(3)	144(7)	52(7)	55(7)	0.080(2)							
	2	0.097(3)	119(17)	135(42)	121(34)	0.083(2)		d					c
	3	0.099(3)	109(22)	46(41)	130(28)	0.106(2)							
Al	1	0.061(4)	118(29)	34(15)	73(24)	0.070(2)				0.054(1)	e	e	e
	2	0.065(4)	43(25)	80(32)	48(19)	0.081(2)		d		0.054(1)	e	e	e
	3	0.074(3)	60(15)	58(12)	133(18)	0.085(2)				0.069(2)	54.7	54.7	54.7
Sp	1	0.057(4)	147(12)	82(9)	59(10)	0.070(1)							
	2	0.071(4)	61(13)	52(13)	51(13)	0.077(1)		d					c
	3	0.082(3)	104(9)	39(12)	126(10)	0.089(1)							
Mn-Gr	1	0.088(3)	155(8)	114(8)	95(7)	0.092(2)				0.087 <sup>f</sup>	54.7	54.7	54.7
	2	0.104(3)	66(9)	154(18)	100(38)	0.104(2)		d		0.089	e	e	e
	3	0.107(3)	90(18)	79(35)	169(34)	0.110(2)				0.089	e	e	e
Gr	1	0.089(3)	166(9)	84(11)	102(9)	0.079(2)				0.077(1)			
	2	0.101(3)	101(13)	150(38)	62(37)	0.088(2)		d		0.097(7)			d
	3	0.104(3)	82(12)	119(39)	149(35)	0.096(1)				0.097(7)			
Uv	1	0.060(6)	155(9)	106(13)	72(8)	0.060(2)				0.026(6)			
	2	0.075(4)	78(14)	161(15)	104(17)	0.065(5)		d		0.067(3)			d
	3	0.089(4)	111(8)	81(17)	156(12)	0.081(5)				0.067(3)			
Go	1	0.089(4)	96(22)	7(24)	87(10)	0.083(3)				0.070			
	2	0.097(4)	25(10)	83(24)	114(8)	0.089(4)		d		0.076			d
	3	0.113(4)	114(8)	90(5)	156(8)	0.100(4)				0.076			
An	1	0.067(5)	151(12)	81(7)	63(10)	0.071(3)							
	2	0.085(2)	63(11)	52(13)	50(14)	0.080(3)		d					c
	3	0.097(4)	100(9)	39(13)	128(11)	0.085(3)							

a. Vibration ellipsoid of Si for all nine garnets is statistically isotropic with an indeterminate orientation. b. r(1), r(2), and r(3) are the ellipsoid axes and X, Y, Z, the crystallographic axes. c. Indeterminate (isotropic) ellipsoid. d. Same as above. e. Indeterminate (uniaxial) ellipsoid. f. Indeterminate e.s.d.'s.

TABLE 9. INTERATOMIC DISTANCES (Å) AND ANGLES (°) OF THE SiO<sub>4</sub> TETRAHEDRON AND YO<sub>6</sub> OCTAHEDRON OF NINE SILICATE GARNETS.

GARNET	Sf-0(1) <sup>a</sup>	0(1)-0(2)	0(1)-0(3)	<0-0>	0(1)-Si-0(2)	0(1)-Si-0(3)	Y-0(1)	0(1)-0(4)	0(1)-0(5)	<0-0>	0(1)-Y-0(4)	0(1)-Y-0(5)
f <sup>b</sup>	4	2	4	4	2	4	6	6	6	6	5	6
Fy	1.634(1) <sup>c</sup>	2.434(2)	2.751(3)	2.665	99.52(9)	114.67(9)	1.886(1)	2.617(3)	2.716(2)	2.667	87.87(6)	92.13(6)
Cr-Py	1.639(1)	2.510(2)	2.757(2)	2.675	99.88(8)	114.47(5)	1.905(1)	2.646(2)	2.743(2)	2.693	88.00(5)	92.00(5)
Al	1.628(2)	2.500(3)	2.737(2)	2.658	100.04(5)	114.38(5)	1.896(2)	2.655(2)	2.708(3)	2.682	88.87(5)	91.13(5)
Sp	1.637(1)	2.520(2)	2.746(2)	2.671	100.67(7)	114.04(4)	1.902(1)	2.678(2)	2.702(2)	2.690	89.48(5)	90.52(5)
Mn-Gr	1.645(1)	2.543(3)	2.755(3)	2.684	101.24(10)	113.74(5)	1.903(1)	2.692(2)	2.686(2)	2.689	90.13(7)	89.87(7)
Gr	1.645(1)	2.557(2)	2.745(1)	2.686	102.53(8)	113.05(4)	1.924(1)	2.756(2)	2.686(2)	2.721	91.46(5)	88.54(5)
Dv	1.643(2)	2.577(4)	2.735(4)	2.682	103.26(9)	112.67(7)	1.985(2)	2.845(4)	2.769(4)	2.807	91.56(7)	88.44(7)
Go	1.655(2)	2.575(4)	2.763(4)	2.700	102.19(8)	113.23(9)	1.988(2)	2.835(4)	2.789(4)	2.812	90.95(10)	89.05(10)
An	1.643(2)	2.564(4)	2.739(3)	2.681	102.64(7)	112.99(8)	2.024(2)	2.890(3)	2.834(4)	2.862	91.12(7)	88.88(7)

a. The numbers in parentheses following an atom designation indicate the atom nomenclature of Figure 3. b. The numbers in this row refer to the frequency of occurrences. c. The numbers in parentheses following a distance or angle are the e.s.d.'s.

TABLE 10. INTERATOMIC DISTANCES (Å) AND ANGLES (°) OF THE XO<sub>3</sub> TRIANGULAR DODECAHEDRON FOR NINE SILICATE GARNETS.

GARNET	X(1)-O(1) <sup>a</sup>	X(2)-O(4)	X(3)-O(5)	O(1)-O(4)	O(4)-O(5)	O(1)-O(7)	O(3)-O(7)	O(1)-X(2)-O(4)	O(1)-X(2)-O(5)	O(4)-X(2)-O(5)	O(4)-X(2)-O(7)	O(1)-X(2)-O(7)	O(3)-X(2)-O(7)	
Py	2.196(2) <sup>c</sup>	2.242(2)	2.269(2)	2.617(3)	2.709(3)	2.782(3)	3.106(1)	3.402(3)	2.929	69.20(7)	70.34(6)	72.86(7)	93.47(4)	109.46(7)
Cr-Py	2.218(1)	2.253(1)	2.284	2.510(2)	2.646(2)	2.726(2)	3.127(1)	3.481(1)	2.950	68.98(5)	70.71(5)	72.52(6)	93.41(3)	109.86(5)
Al	2.220(1)	2.278(1)	2.300	2.500(2)	2.655(2)	2.768(2)	3.133(1)	3.494(2)	2.948	68.38(8)	70.44(8)	72.20(5)	92.85(4)	110.08(5)
Sp	2.247(1)	2.408(2)	2.328	2.520(2)	2.678(2)	2.824(3)	3.167(1)	3.553(2)	3.004	68.21(5)	70.34(5)	71.75(4)	92.56(4)	110.40(5)
Mn-Sp	2.257(2)	2.438(2)	2.353	2.543(3)	2.688(3)	2.843(3)	3.197(1)	4.008(3)	3.026	68.17(7)	69.67(6)	71.43(4)	92.31(4)	110.54(5)
Gr	2.219(1)	2.480(1)	2.405	2.567(2)	2.758(2)	2.973(2)	3.450(1)	4.121(2)	3.101	67.20(5)	69.84(4)	70.27(6)	91.61(4)	111.66(6)
Gr	2.260(2)	2.499(2)	2.429	2.577(4)	2.844(2)	2.968(4)	3.481(2)	4.169(4)	3.131	66.18(9)	71.61(8)	69.31(8)	91.46(5)	113.01(9)
Go	2.244(3)	2.501(2)	2.425	2.575(4)	2.835(4)	2.871(5)	3.480(2)	4.153(5)	3.126	66.50(11)	71.48(10)	70.09(11)	91.67(7)	112.27(11)
An	2.266(2)	2.505(2)	2.433	2.584(4)	2.860(3)	2.936(4)	3.495(2)	4.174(3)	3.134	65.84(10)	72.82(10)	69.43(9)	91.44(5)	113.25(9)

a. The numbers in parentheses following an atom designation indicate the atom nomenclature of Figure 3. b. The numbers in this row refer to the frequency of occurrences. c. The numbers in parentheses following a distance or angle are the s.d.'s.

TABLE 11. METAL-METAL INTERATOMIC DISTANCES (Å) FOR NINE SILICATE GARNETS

Garnet	X-Y	X(2)-Si	X(1)-Si	Y-Si	X(1)-X(2)	Si-Si	Y-Y
f <sup>a</sup>	4	2	4	6	4	4	8
Py	3.201	3.507	2.863	3.201	3.507	3.507	4.945
Cr-Py	3.222	3.529	2.882	3.222	3.529	3.529	4.991
Al	3.223	3.531	2.883	3.223	3.531	3.531	4.993
Sp	3.248	3.558	2.905	3.248	3.558	3.558	5.032
Mn-Gr	3.268	3.579	2.923	3.268	3.579	3.579	5.062
Gr	3.311	3.627	2.961	3.311	3.627	3.627	5.129
Uv	3.351	3.671	2.997	3.351	3.671	3.671	5.191
Go	3.357	3.678	3.003	3.357	3.678	3.678	5.201
An	3.370	3.692	3.015	3.370	3.692	3.692	5.221

<sup>a</sup> The numbers in this row refer to the frequency of occurrences.

*The SiO<sub>4</sub> Tetrahedron.* The Si-O bond length in the silicate garnets does not show a lengthening with increased average electronegativity of the nontetrahedral cations,  $\bar{\chi}$ , as found for the *C2/m* amphiboles (Brown and Gibbs, 1969). In fact, it decreases slightly as  $\bar{\chi}$  increases. In a concurrent and similar study of eleven olivines (Brown, 1970; Brown and Gibbs, in press), the length of the Si-O bond was also found to decrease slightly with increasing  $\bar{\chi}$ . These trends are consistent with Raman spectroscopic studies by Griffith (1969) who suggests that Si-O bond lengths in orthosilicates are controlled by structural rather than electronegativity factors.

The mean Si-O bond length for these garnets (1.64 Å) is in agreement with that of other silicates with 4-coordinated oxygens (1.638 Å) (Brown and Gibbs, 1969; and Shannon and Prewitt, 1969). Gibbs and Smith (1965) suggested that Si-O bond lengths for silicate garnets will be within  $\pm 0.005$  of 1.63 Å. Their prediction is in agreement for garnets with

TABLE 12. OBSERVED ANGLES ABOUT OXYGEN (°), M-O-M, FOR NINE SILICATE GARNETS

Garnet	Y-O-Si	Y-O-X(2)	Y-O-X(2)	X(1)-O-Si	X(2)-O-Si	X(1)-O-X(2)	M-O-M
Py	130.76 (7) <sup>a</sup>	103.04 (6)	97.85 (6)	95.64 (7)	122.77 (7)	101.14 (5)	108.53
Cr-Py	130.60 (7)	102.60 (5)	97.81 (4)	95.57 (5)	123.28 (6)	101.11 (4)	108.49
Al	132.10 (8)	102.78 (6)	97.23 (9)	95.79 (9)	122.47 (8)	100.25 (5)	108.35
Sp	133.08 (7)	102.72 (4)	97.11 (5)	95.55 (5)	122.05 (6)	99.65 (4)	108.37
Mn-Gr	134.34 (9)	102.83 (7)	96.98 (5)	95.30 (5)	121.24 (7)	98.94 (6)	108.24
Gr	135.95 (7)	102.19 (7)	96.33 (4)	95.14 (6)	121.20 (6)	97.83 (5)	108.08
Uv	134.70 (10)	100.58 (8)	96.03 (8)	95.28 (9)	123.39 (11)	98.02 (6)	108.02
Go	134.17 (15)	101.15 (9)	96.14 (10)	95.63 (9)	123.18 (12)	98.57 (9)	108.14
An	133.37 (10)	100.03 (8)	95.75 (8)	95.86 (10)	124.77 (10)	98.68 (6)	108.08

<sup>a</sup> The numbers in parentheses are the e.s.d.'s and refer to the last figure quoted.

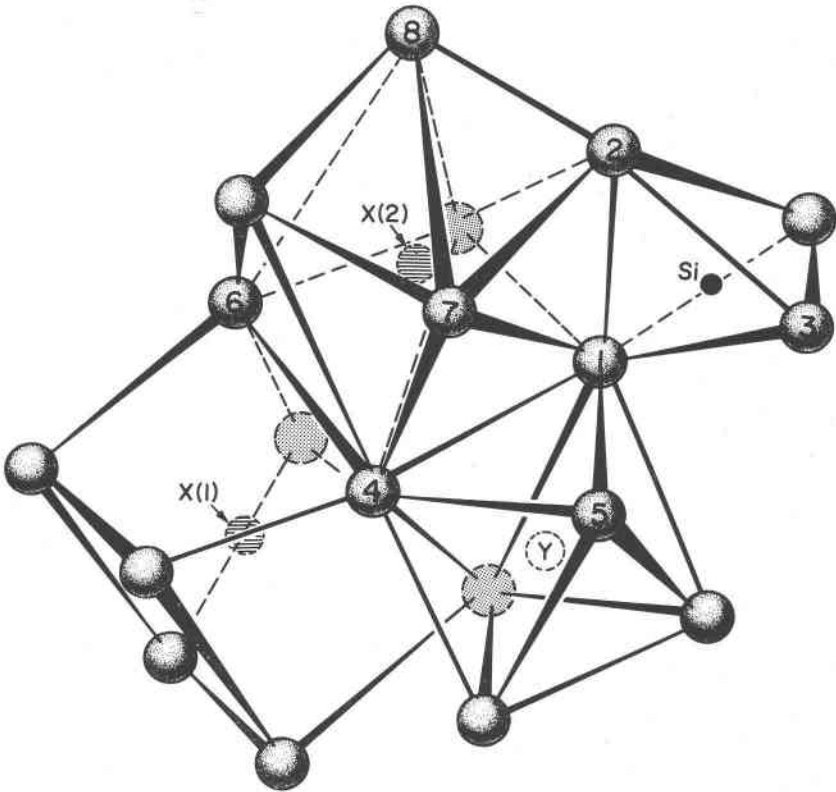


FIG. 3. Portion of the garnet structure with cation and oxygen atoms labeled in accordance with the nomenclature of Tables 9-15.

$\langle r\{X\} \rangle$  less than  $1.0 \text{ \AA}$ ; however, application of a chi-square test to the garnet data indicates two populations of Si-O bond lengths for the silicate garnets, the second being  $1.65 \text{ \AA} \pm 0.005$  for garnets with  $\langle r\{X\} \rangle$  greater than  $1.0 \text{ \AA}$ . Geller (1967) correctly observed that variations in Si-O bond lengths could be greater than the  $\pm 0.005 \text{ \AA}$  proposed by Gibbs and Smith (1965).

The size effect of the  $\{X\}$  cation on the tetrahedron is seen in Figure 5A, where the tetrahedral bond angle strain of the angle opposite the shared edge,  $[O(1)\text{-Si-O}(2)] - 109.47^\circ$  (Table 13), is plotted against  $\langle r\{X\} \rangle$  for the Al garnets. The  $\text{SiO}_4$  tetrahedron in garnet becomes linearly more regular as  $\langle r\{X\} \rangle$  increases. The bond angle strain of the unshared edge,  $[O(1)\text{-Si-O}(3)] - 109.47^\circ$ , shows the same linear trend, though less pronounced (see Table 13). There is little change in the bond angle strain with respect to  $\langle r\{Y\} \rangle$  for the Ca garnets. The trend of decreasing distor-

TABLE 13. POLYHEDRAL DISTORTIONS FOR NINE SILICATE GARNETS.

GARNET	$\sigma$	$\sigma_{\phi}$	$\phi$	BOND STRAIN ( $\text{\AA}$ )		ANGULAR DIFFERENCES (BOND ANGLE STRAINS) ( $^{\circ}$ )							
				$\frac{[O(1)-O(3)]}{-[O(1)-O(2)]}$	$\frac{[O(1)-O(5)]}{-[O(1)-O(4)]}$	$[O(1)-Si-O(2)]$	$[O(1)-Si-O(3)]$	$[O(1)-T-O(4)]$	$[O(1)-X(2)-O(2)]$	$[O(1)-X(2)-O(4)]$	$\frac{[O(4)-X(2)-O(6)]}{-71.70}$	$\frac{[O(4)-X(2)-O(7)]}{-71.70}$	
Py	53.2	1.5	3.4	0.257	0.099	-9.95	5.20	-90.00 $^{\circ}$	-2.13	-0.25	0.89	1.52	1.16
Cr-Fy	53.3	1.4	3.4	0.247	0.094	-9.59	5.00	-2.00	-2.00	-0.47	1.26	1.38	0.82
Al	53.9	0.6	3.8	0.237	0.053	-9.43	4.91	-1.13	-1.13	-1.07	0.99	2.24	0.50
Sp	54.3	0.4	3.9	0.226	0.025	-8.81	4.58	-0.55	-0.55	-1.24	0.69	2.89	0.05
Mn-Gr	54.8	-0.1	4.1	0.221	-0.006	-8.23	4.27	0.13	0.13	-1.28	0.10	3.75	-0.27
Gr	55.6	-1.1	4.0	0.178	-0.070	-6.59	3.58	1.46	1.46	-2.25	0.39	4.58	-1.43
Uv	55.9	-1.2	3.2	0.158	-0.076	-6.21	3.20	1.57	1.57	-3.27	2.16	3.54	-2.39
Go	55.4	-0.7	3.5	0.187	-0.045	-6.38	3.74	0.97	0.97	-2.95	2.03	3.17	-1.61
An	55.5	-0.6	3.0	0.175	-0.056	-6.83	3.58	1.12	1.12	-3.81	3.37	2.47	-2.27

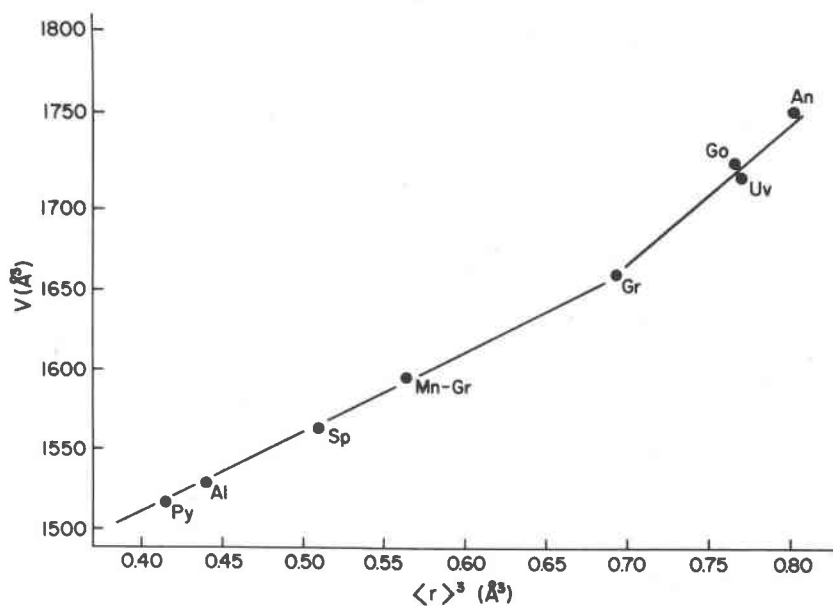


FIG. 4. Variation of the cell volumes,  $V(\text{\AA}^3)$ , for eight silicate garnets with respect to the cubed mean radius,  $\langle r \rangle^3$ , of the non-tetrahedral cations. In this figure and all subsequent ones representing correlations, the size of the data plots is greater than the magnitude of the e.s.d.'s.

tions from the pyrospites to the ugrandites agrees well with those predicted by Born and Zemann (1964) and Moore, White, and Long (1969). However, increasing the regularity of the  $\text{SiO}_4$  tetrahedron with the size of the  $\{X\}$  cation should permit the  $sp^3$ -hybrid orbitals on oxygen to be in a position for a more favorable overlap with those of Si, suggesting a decrease in the Si-O bond length (Fyfe, 1954) as the tetrahedron becomes more regular. This is not the case, for as it becomes more regular, the Si-O bond length actually increases. This increase may be due to a simple stretching of the  $[\text{Al}_2](\text{Si}_3)\text{O}_{12}$  framework in response to the increasing  $\langle r\{X\} \rangle$ .

Born and Zemann (1964) discuss the position angle,  $\alpha$ , of the  $\text{SiO}_4$  tetrahedron with respect to the crystallographic axes for the Al-garnets. From their geometrical analysis they predict  $\alpha$  values for almandine and spessartine to be intermediate between those of pyrope ( $\alpha = 28.3^\circ$ ) and grossular ( $\alpha = 25.4^\circ$ ). Values of  $\alpha$  of  $27.4^\circ$  for almandine and  $27.0^\circ$  for spessartine substantiate their predictions.

*The  $\text{YO}_6$  Octahedron.* The  $\text{YO}_6$  octahedron in the silicate garnets is more

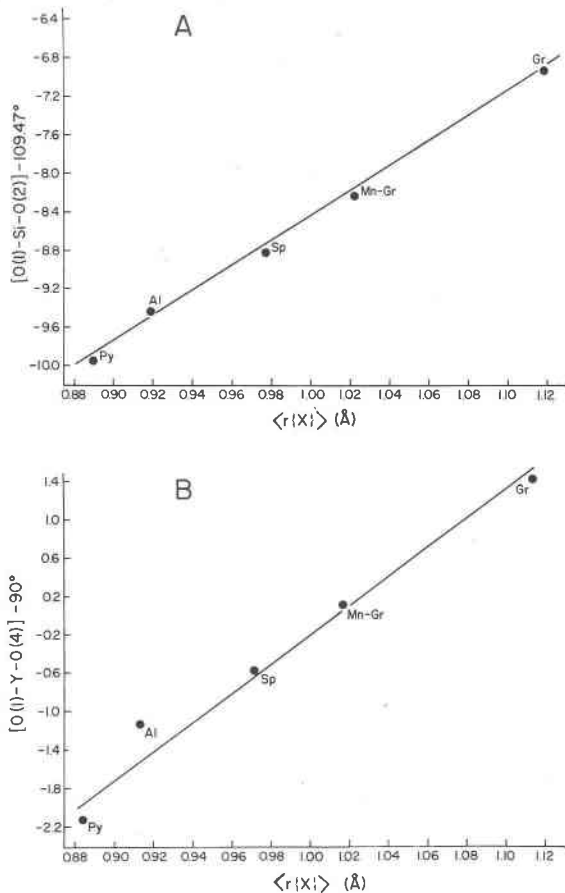


FIG. 5. Tetrahedral bond angle strain of the angle opposite the shared edge,  $[O(1)-Si-O(2)]-109.47^\circ$ , for the Al garnets plotted against  $\langle r\{X\} \rangle$  (A). Octahedral bond angle strain,  $[O(1)-Y-O(4)]-90.0^\circ$ , plotted against  $\langle r\{X\} \rangle$  for the Al garnets (B).

regular than the  $SiO_4$  tetrahedron. Like the Si-O bond, the Al-O bond length for the  $[Y]=Al$  garnets, shows two populations:  $1.895 \pm 0.01 \text{ \AA}$  for  $\langle r\{X\} \rangle$  less than  $1.10 \text{ \AA}$ , but  $1.924 \text{ \AA}$  for grossular. Zemann (1962) anticipated two Al-O bond length populations in his discussion of ideal silicate garnets, one with Al-O =  $1.90 \text{ \AA}$  and the other with Al-O =  $1.95 \text{ \AA}$ . However, for the Ca garnets, the Y-O bond lengths agree well with the sum of Shannon and Prewitt's radii for  $[Y]$  and  $IV_O$ . Accordingly, the Y-O bond lengths for these garnets vary linearly with  $\langle r\{Y\} \rangle$  (Figure 6A) unlike the Al garnets where  $\langle r\{Y\} \rangle$  is essentially constant.

One anomalous feature of the silicate garnets with  $\{X\} = Ca$  is that

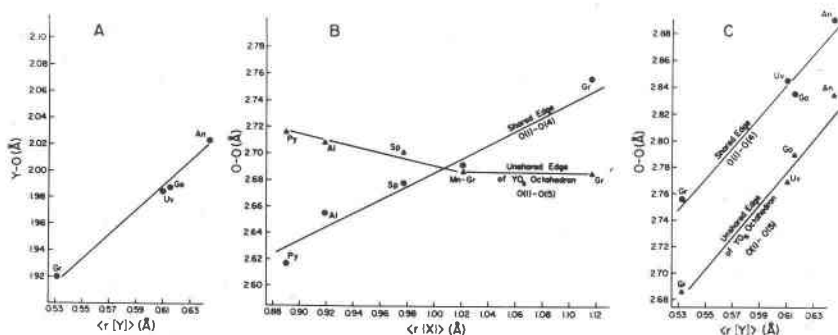


FIG. 6. Y-O bond distance plotted against  $\langle r\{Y\} \rangle$  for the Ca garnets (A). Shared octahedral edge, O(1)-O(4), and unshared octahedral edge, O(1)-O(5), plotted against  $\langle r\{X\} \rangle$  for the Al garnets (B) and against  $\langle r\{Y\} \rangle$  for the Ca garnets (C).

the octahedral edge shared with the triangular dodecahedron, O(1)-O(4), is significantly longer than the unshared octahedral edge, O(1)-O(5). Figures 6B, C are plots of these edge lengths versus  $\langle r\{X\} \rangle$  for the Al garnets, and versus  $\langle r\{Y\} \rangle$  for the Ca garnets, respectively. As  $\langle r\{X\} \rangle$  increases from pyrope (Py) to grossular (Gr), the shared edge increases linearly while the unshared edge decreases in length. The shared edge also varies linearly with the metal-metal X-Y distance, increasing from 2.68 to 2.90 Å as X-Y increases from 3.20 to 3.36 Å. Geller (1967) has predicted that it should be possible for a silicate garnet with an X-cation intermediate in size between Mg and Ca to possess a regular octahedron. This is the case for Mn-grossular (Mn-Gr) where shared and unshared octahedral edge lengths are statistically identical. From pyrope to spessartine, cation-cation repulsions across the shared edges may be so strong (perhaps because the X-Y metal-metal distance (3.20–3.25 Å) is sufficiently short to enhance these repulsions) that the shared edges are shorter than the unshared edges. However, an increase in  $\langle r\{X\} \rangle$  not only increases the length of the shared edge and the X-Y distance (thus weaker cation-cation repulsions across the shared edge), but also forces the two oxygens of the unshared edge closer together until they are 2.686 Å apart in Mn-grossular. A further increase in  $\langle r\{X\} \rangle$  from 1.022 to 1.118 Å leaves this length unchanged. Anion-anion, non-bonding, closed-shell repulsions apparently are sufficient to counteract any further decrease. Thus, the value of 2.68 Å appears to be near the lower limit of O-O distances for an unshared octahedral edge in the silicate garnets. In kyanite there are two unshared Al-octahedral edges that are 2.683 and 2.674 Å long (Burnham, 1963). Although it appears possible to have one or two unshared edges shorter than 2.68 Å, any more would probably

lower the stability of the octahedron. Therefore, as garnet has six unshared octahedral edges, it is unlikely that they will fall below 2.68 Å without introducing strong destabilizing, non-bonding, closed-shell repulsions.

For silicate garnets with shared octahedral edges shorter than unshared ones, the octahedral cavity is elongated parallel to its  $S_6$  axis and the vibration spheroid of the [Y] cation is prolate in conformity with the cavity, with its major axis parallel to  $S_6$ . On the other hand, those garnets with unshared octahedral edges longer than shared ones have octahedral cavities that are flattened parallel to their  $S_6$  axis, and the vibration spheroid is oblate in conformity with the cavity, with its minor axis parallel to  $S_6$ . For Mn-grossular, which has a nearly regular octahedron, the [Y] cation is statistically spherical in its thermal vibration. The relationship between the octahedral shared and unshared edge lengths is directly evinced in the bond angle strain for the shared edge [O(1)-Y-O(4)]—90°, plotted in Figure 5B against  $\langle r\{X\} \rangle$ . The octahedral distortion of pyrope and grossular are, except for a change in sign, quite similar (see also Table 13 and Figure 6B).  $AlO_6$  octahedra with similar distortions should also have similar Al-O distances. However, this is not the case, as Al-O = 1.886 Å for pyrope but 1.924 Å for grossular. The 2.5 percent  $Fe^{3+}$  in the [Y] site of grossular is insufficient to produce the significantly longer Al-O distance. In fact, adding 2.5 percent  $Fe^{3+}$  to the [Y] site of pyrope would only increase the Al-O distance to about 1.89 Å,  $\sim 0.035$  Å less than the Al-O of grossular. The increase in  $\langle r\{X\} \rangle$  appears to expand the  $[Al_2](Si_3)O_{12}$  framework, with the regularity of the octahedron having little effect on variations in the Al-O bond length. If it did, Mn-grossular, with the most regular octahedron, would have the shortest Al-O bond length; however, its length is statistically identical to that found in pyrope.

Octahedral bond angle strain for the Ca garnets is nearly constant relative to  $\langle r\{Y\} \rangle$ , and thus the distortion of the octahedra appears to be independent of the electron configuration of the transition metal [Y] cations, *i.e.*,  $Cr^{3+}$ ,  $V^{3+}$ , or  $Fe^{3+}$ . Abrahams and Geller (1957) predicted that uvarovite and andradite should have successively more regular octahedra than grossular. However, according to criteria based on the quadratic elongation (Robinson, Gibbs, and Ribbe, *in press*), the octahedron in grossular is more regular than that in uvarovite but less so than that in andradite. In fact, the octahedra in the garnets are more regular than those in the olivines, the humites, the pyroxenes and the amphiboles. Finally, the average dimensions of the octahedron in terms of mean edge length,  $\langle O-O \rangle$ , (Table 9) are nearly constant for the Al garnets, but show a slight linear increase for the Ca garnets with respect to increasing  $\langle r\{Y\} \rangle$ .

*The  $XO_8$  Triangular Dodecahedron.* The 8-fold coordination polyhedron about the  $X$ -cation can best be described as a slightly distorted triangular dodecahedron, because observed O-O-O and O-X-O angles deviate only a few degrees from ideal triangular dodecahedral angles (Lippard and Russ, 1968). Bond angle strains are considerably larger if the 8-fold polyhedron is characterized as a cube or a square antiprism. Furthermore, the cube and antiprism are less favorable polyhedra from the standpoint of anion-anion, non-bonding repulsions than are dodecahedra (Lippard and Russ, 1968). The two unique X-O distances,  $X(1)$ -O and  $X(2)$ -O, as well as their mean,  $\langle X-O \rangle$ , increase linearly with  $\langle r\{X\} \rangle$  for the Al garnets (Figure 7A). The bond length of  $X(1)$ -O is about 0.2 Å shorter than that of  $X(2)$ -O for all the silicate garnets. Zemann (1962) argued that X-Si cation repulsions across the shared edge should result in  $X(1)$ -O being longer than  $X(2)$ -O. As this is not the case, Zemann concluded that this is a result of unshared dodecahedral edges being of necessity longer than 2.75 Å. Since none of the silicate garnets studied have unshared dodecahedral edges less than 2.78 Å, Zemann's explanation is plausible. Alternatively, if the valence electrons of  $\{X\}$  can be  $d^4sp^8$  hybridized (Kimball, 1940), it is expected from theoretical considerations that  $X(1)$ -O bonds in a triangular dodecahedron will be shorter than  $X(2)$ -O bonds

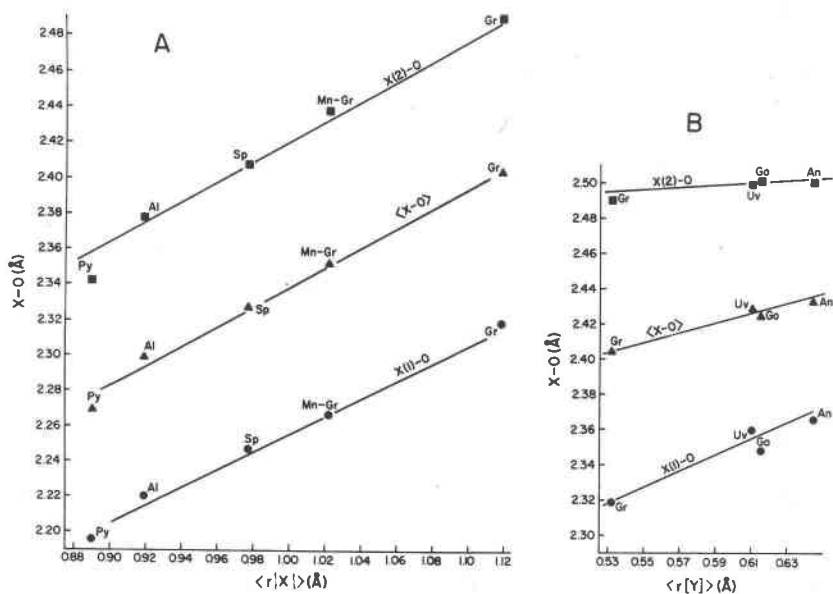


FIG. 7. Metal-oxygen distances,  $X(1)$ -O,  $X(2)$ -O, and their mean,  $\langle X-O \rangle$ , of the triangular dodecahedron plotted against  $\langle r\{X\} \rangle$  for the Al garnets (A) and against  $\langle r\{Y\} \rangle$  for the Ca garnets (B).

(Hoard and Silverton, 1963). Gibbs and Smith (1965) found no reason to invoke orbital hybridization for the dodecahedron in pyrope and concluded from a geometrical analysis that if  $X(2)$ -O is longer than  $X(1)$ -O, the result is unreasonable Y-O and O-O unshared edge lengths, a conclusion similar to Zemann's (1962).

The  $X(1)$ -O bond length in those garnets where  $\{X\} = \text{Ca}$  shows the same rate of linear increase with respect to  $\langle r[Y] \rangle$  (Figure 7B) as it shows with increasing  $\langle r\{X\} \rangle$  for the  $[Y] = \text{Al}$  garnets (Figure 7A). On the other hand, the  $X(2)$ -O length in the Ca garnets is essentially constant with respect to  $\langle r[Y] \rangle$ . The mean X-O bond length,  $\langle X-O \rangle$ , thus shows a linear increase with respect to  $\langle r[Y] \rangle$ , which indicates that the effective radius of Ca is not constant, but is  $\sim 0.03 \text{ \AA}$  larger in andradite than in grossular.

The triangular dodecahedron has three types of shared polyhedral edges (see Table 1). The two symmetrically equivalent edges shared with  $\text{SiO}_4$  tetrahedra and the four shared with  $\text{YO}_6$  octahedra have already been examined. It also has four equivalent edges common with other triangular dodecahedra, O(4)-O(6), as well as eight unshared edges; one set of two, O(4)-O(7), is nearly equal to the length of the shared edge between dodecahedra, and two sets, one of two, O(1)-O(7), and one of four, O(8)-O(7), which are considerably longer than the shared edge (see Table 10). The shared dodecahedral edge and its shortest unshared edge are plotted against  $\langle r\{X\} \rangle$  and  $\langle r\{Y\} \rangle$  in Figures 8A and 8B. For pyrope (Py) the shared edge is shorter than the unshared one, but as  $\langle r\{X\} \rangle$  increases, both edges increase linearly in length, with the shared edge increasing faster than the unshared one. For spessartine (Sp) the shared edge equals the unshared, whereas it is actually longer than the unshared edge in Mn-grossular and grossular. Both show a slight decrease in length with increasing  $\langle r[Y] \rangle$  as seen in Figure 8B, but again the shared edge is longer than the unshared. In the Ge garnet,  $\{\text{Mn}_3\}[\text{Fe}_2](\text{Ge}_3)\text{O}_{12}$ , the shared edge,  $2.766 \text{ \AA}$ , is significantly shorter than the unshared,  $2.921 \text{ \AA}$  (Lind and Geller, 1969). This suggests that Ge in tetrahedral coordination expands the framework, permitting Mn to be more easily accommodated in the structure without resulting in shared edges longer than unshared ones. The average dimensions of the triangular dodecahedral edges,  $\langle \text{O-O} \rangle$ , increase linearly across the series from pyrope to grossular with respect to  $\langle r\{X\} \rangle$  (Fig. 8C) and show an increase that is identical to that of  $\langle X-O \rangle$  as  $\langle r[Y] \rangle$  increases for the Ca garnets (Table 12).

For an ideal triangular dodecahedron, there are two unique O-X-O angles of  $69.45^\circ$  and  $71.70^\circ$  (Lippard and Russ, 1968). Bond angle strains vary linearly with respect to  $\langle r\{X\} \rangle$  and  $\langle r[Y] \rangle$  for the two garnet series and are given in Table 13 for the angles opposite the edge (a) shared with a tetrahedron,  $[\text{O}(1)-X(2)-\text{O}(2)] - 69.45^\circ$ , (b) shared with an octahedron,

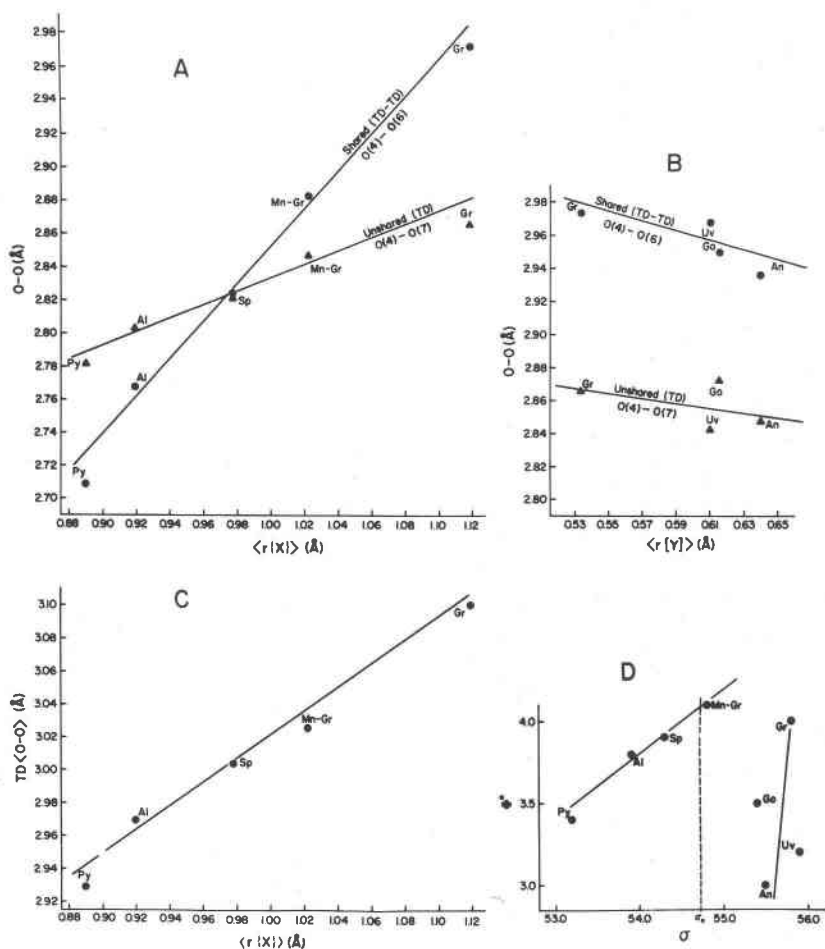


FIG. 8. Triangular dodecahedral shared edge length, O(4)-O(6), and unshared edge length, O(4)-O(7), plotted against  $\langle r\{X\} \rangle$  for the Al garnets (A) and against  $\langle r\{Y\} \rangle$  for the Ca garnets (B). Mean triangular dodecahedral edge length, TD(O-O), plotted against  $\langle r\{X\} \rangle$  for the Al garnets (C). Tetrahedral-octahedral distortion parameter  $\beta$  plotted against the dodecahedral distortion parameter  $\phi$  (D).

[O(1)-X(2)-O(4)]-69.45°, (c) shared with a dodecahedron, [O(4)-X(2)-O(6)]-71.70°, and for (d) the angle opposite the shortest unshared edge [O(4)-X(2)-O(7)]-71.70°. For those garnets with [Y]=Al, all bond angle strains show a decrease (0.5 to 2.0°) with increasing  $\langle r\{X\} \rangle$  except for the angle opposite the edge shared with another dodecahedron, which increases  $\sim 3^\circ$ . For those garnets with  $\{X\} = \text{Ca}$ , all angle strains show a

linear decrease (1 to 2°) with  $\langle r[Y] \rangle$ , except for the angle opposite the octahedrally shared edge which also increases  $\sim 3^\circ$ .

*Comparison of Polyhedral Distortions.* Euler and Bruce (1965) have defined two functions,  $\sigma$  and  $\Phi$ , which they indicate can be related to tetrahedral-octahedral and tetrahedral-dodecahedral distortions in the garnets. Figure 8D is a plot of  $\sigma$  versus  $\Phi$  for eight of the silicate garnets studied, where  $\sigma_0$  is the ideal angle of  $54.73^\circ$  between the  $Y-O$  bond and a vector constructed normal to an octahedral face and where  $\Phi$  is the angle between the  $[1\bar{1}0]$  and the projection of the  $Y-O$  bond on the (111). A multiple linear regression analysis for the silicate garnet data shows  $\sigma$  to be highly correlated ( $\hat{R}_1(\sigma)=0.998$ ) with octahedral bond angle strain, and somewhat less so ( $\hat{R}_1(\sigma)=0.974$ ) with tetrahedral bond angle strain. However, the regression analysis shows  $\Phi$  to be nearly independent ( $\hat{R}_1(\Phi)=0.255$ ) of tetrahedral bond angle strain, but highly correlated ( $\hat{R}_1(\Phi)=0.988$ ) with dodecahedral bond angle strains. It appears, at least for the silicate garnets, that  $\sigma$  is a good measure of tetrahedral-octahedral distortion and that  $\Phi$  is a good measure of dodecahedral distortion, but not of tetrahedral distortion.

Figure 8D is independent of cell edge and choice of cation radii and supports Winchell's (1933) division of silicate garnets into pyralspites and ugrandites. The pyralspites display a trend of increasing regularity of the octahedron and tetrahedron and decreasing regularity of the dodecahedron from pyrope to spessartine. For the ugrandites, the dodecahedron becomes more regular, but the octahedron and tetrahedron show little change from grossular to andradite. These trends are consistent with the bond angle strains of the respective polyhedra (see Table 13).

Besides the characteristic trend of the pyralspites in Figure 8D, it appears that they are also distinguished from the ugrandites by possessing shorter Si-O bond lengths, as well as shared edges which are shorter than unshared ones. If Cr-pyrope were included in Figure 8D, it would plot close to pyrope. Furthermore, it possesses an Si-O bond length and other structural features that are characteristic of pyralspites. On the other hand, goldmanite plots with the ugrandites and has structural features which are characteristic of them. Although Mn-grossular plots with the pyralspites, it has structural features that are characteristic of both groups and is considered to be an intermediate member.

*Oxygen Positional Parameters and Cation Radii.* It is apparent that not only the cell edges but many of the bond lengths and angles in the silicate garnets can be linearly related to  $\langle r\{X\} \rangle$  and  $\langle r[Y] \rangle$ . Zemann (1962)

obviously realized this when he predicted that the cell edges and bond lengths and angles in almandine and spessartine are intermediate between those in pyrope and grossular. As the bond lengths and angles in garnet are determined in part by the positional parameters of oxygen (the cations are in special positions), it was reasoned that these positional parameters might also be linearly dependent on  $\langle r\{X\} \rangle$  and  $\langle r[Y] \rangle$ . Accordingly, a multiple linear regression analysis was undertaken for the nine garnets to test this reasoning. The calculation yielded the following equations in terms of the Shannon and Prewitt's (1969) effective radii:

$$x = 0.0059(5) + 0.022(2)\langle r\{X\} \rangle + 0.014(5)\langle r[Y] \rangle \quad (3)$$

$$y = 0.0505(4) - 0.023(2)\langle r\{X\} \rangle + 0.037(4)\langle r[Y] \rangle \quad (4)$$

$$z = 0.6431(7) - 0.009(3)\langle r\{X\} \rangle + 0.034(7)\langle r[Y] \rangle \quad (5)$$

where  $\hat{R}_1(x)=0.99$ ,  $\hat{R}_1(y)=0.98$ , and  $\hat{R}_1(z)=0.88$ ; the e.s.d.'s are given in parentheses and refer to the last figure stated. The multiple linear correlation coefficients indicate that approximately 97 percent of the variation of  $x$  and  $y$  can be explained in terms of a linear dependence on  $\langle r\{X\} \rangle$  and  $\langle r[Y] \rangle$ , whereas about 80 percent of the variation of  $z$  can be similarly explained. Because of this high linear dependence, it should be possible to predict the positional parameters of oxygen solely in terms of the chemical composition of a cubic silicate garnet.

To ascertain the internal consistency of the regression equations and equation (1), the cell edges and oxygen positional parameters for Fe-pyrope (Euler and Bruce, 1965) and grossular (Prandl, 1966) were predicted and are compared with the observed values in Table 14. The positional parameters for both garnets and the cell edge for grossular are identical with those observed, whereas the cell edge predicted for Fe-pyrope shows a discrepancy of about 0.05 Å. However, since the data for Fe-pyrope are in close agreement with the pyralspite trend in Figure 8D, which is independent of the choice of radii and cell edge, and deviate significantly from the linear plot of cell volume vs.  $\langle r \rangle_8$  (Fig. 4), it is suggested that the cell edge of this garnet is in error. In spite of this discrepancy, all bond lengths and angles calculated with the predicted cell edges and positional parameters are statistically identical with those observed for both minerals.

To learn whether or not the regression equations are applicable to cubic silicate garnets with values of  $\langle r\{X\} \rangle$  and  $\langle r[Y] \rangle$  outside the range of values used in their derivation, the cell edges, oxygen positional parameters, and selected bond lengths and angles of twenty possible silicate garnets are predicted (Table 15). The predicted structures of the

TABLE 14. PREDICTED AND OBSERVED STRUCTURAL DATA FOR GROSSULAR AND Fe-PYROPE

	Grossular		Fe-Pyrope	
	$\{Ca_{2.87}Mg_{0.12}Mn_{0.01}\}[Al_{1.85}Fe_{0.15}](Si_3)O_{12}$		$\{Mg_{1.6}Fe_{1.2}Ca_{0.2}\}[Al_2](Si_3)O_{12}$	
	Observed <sup>a</sup>	Predicted	Observed <sup>b</sup>	Predicted
$a(\text{\AA})$	11.855 (1)	11.85	11.556 (4)	11.51
$x$	0.0381 (1)	0.0380	0.0339 (5)	0.0336
$y$	0.0458 (1)	0.0459	0.0491 (6)	0.0491
$z$	0.6512 (1)	0.6515	0.6535 (6)	0.6530
Si-O(1) <sup>d</sup>	1.651 (2) $\text{\AA}$	1.65	1.635 (7)	1.64
O(1)-O(2)	2.581 (3)	2.58	2.502 (14)	2.50
O(1)-O(3)	2.753 (3)	2.75	2.750 (11)	2.75
O(1)-Si-O(2)	102.8 (1) <sup>o</sup>	102.9	99.8 (4)	99.9
O(1)-Si-O(3)	112.9 (1) <sup>o</sup>	112.9	114.5 (5)	114.5
Y-O(1)	1.927 (2) $\text{\AA}$	1.93	1.903 (7)	1.89
O(1)-O(4)	2.755 (3)	2.76	2.658 (11)	2.64
O(1)-O(5)	2.695 (3)	2.69	2.724 (13)	2.71
O(1)-Y-O(4)	91.3 (1) <sup>o</sup>	91.3	88.6 (4)	88.5
X(1)-O(4)	2.325 (2) $\text{\AA}$	2.32	2.222 (6)	2.21
X(2)-O(4)	2.492 (2)	2.49	2.377 (7)	2.37
$\langle X-O \rangle$	2.408	2.41	2.300	2.29

<sup>a</sup> Data from Prandl (1966).

<sup>b</sup> Data from Euler and Bruce (1965).

<sup>c</sup> The numbers in parentheses following the observed values are the e.s.d.'s.

<sup>d</sup> The numbers in parentheses following an atom designation refer to the nomenclature of Figure 3.

first thirteen garnets in Table 15 show no apparent anomalies: Si-O bond lengths (1.63-1.65  $\text{\AA}$ ) agree with those recorded for other silicates with 4-coordinated oxygens; all shared edges are shorter than unshared edges; tetrahedra and octahedra have distortions compatible with the pyrope garnets; and the sum of Shannon and Prewitt's radii, (Y+O) and (X+O), are similar to the predicted values, Y-O and  $\langle X-O \rangle$ , respectively. Thus, the structures of these garnets are reasonable when compared with other silicate garnets and if the requisite temperatures, pressures, and oxidation states can be obtained, their synthesis should be possible. In fact, under high pressure conditions Coes (1955) has synthesized three of these garnets, namely,  $\{Mg_3\}[Cr_2](Si_3)O_{12}$  (knorringite),  $\{Mg_3\}[Fe_2](Si_3)O_{12}$  (kharite), and  $\{Mn_3\}[Fe_2](Si_3)O_{12}$  (calderite) and Kohn and Eckhart (1962) have synthesized another,  $\{Co_3\}[Al_2](Si_3)O_{12}$ . Gentile and Roy (1960) have synthesized the garnet  $\{Cd_3\}[Al_2](Si_3)O_{12}$  "dry" at one atmosphere. As expected, its predicted structural properties are intermediate between those of Mn-grossular and grossular,



and are characteristically ugrandite where the shared octahedral edge is longer than the unshared one. Also, the size of the octahedral and dodecahedral cavities are compatible with the sum of Shannon and Prewitt's radii.

$\{\text{Sr}_3\}[\text{Al}_2](\text{Si}_3)\text{O}_{12}$  and  $\{\text{Ba}_3\}[\text{Al}_2](\text{Si}_3)\text{O}_{12}$  have a number of anomalous features in their predicted structures: (1) the unshared octahedral edges would be less than 2.68 Å—the value believed to be the minimum for an unshared octahedral edge without introducing strong, destabilizing, anion-anion repulsions; (2) the sum of the radii,  $(X+O)$ , would be significantly greater than the predicted  $X-O$  distances—this indicates that the dodecahedral cavities are too small to stably accommodate the larger  $\{X\}$  cations; and (3) the predicted  $Y-O$  distances would be more than 0.05 Å larger, on the average, than the radius sum  $(Y+O)$ —this indicates that the  $[Y]$  cation is too small to form a bond with each of the oxygen ligands without introducing destabilizing, anion-anion repulsions evinced by the short unshared edges predicted for the octahedron. These anomalies may explain why Gentile and Roy (1960) were unsuccessful in synthesizing garnets of these compositions.

Finally, for compositions having  $\{X\} = \text{Ca}$ , but  $[Y^{3+}] = \text{Ga}$ ,  $\text{Mn}$ ,  $\text{Sc}$ , and  $\text{In}$ , the predicted structures show no anomalies and are similar to those of the ugrandites. Under hydrothermal conditions, Mill (1964 and 1966) has been successful in synthesizing three of these, namely,  $\{\text{Ca}_3\}[\text{Ga}_2](\text{Si}_3)\text{O}_{12}$ ,  $\{\text{Ca}_3\}[\text{Sc}_2](\text{Si}_3)\text{O}_{12}$  and  $\{\text{Ca}_3\}[\text{In}_2](\text{Si}_3)\text{O}_{12}$ , and it appears likely that synthesis of  $\{\text{Ca}_3\}[\text{Mn}_2](\text{Si}_3)\text{O}_{12}$  should also be possible.

*A Structural "Stability" Field for Cubic Silicate Garnets.* It is evident that regression equations predict plausible structural parameters for silicate garnets with a relatively wide range of  $\langle r\{X\} \rangle$  and  $\langle r\{Y\} \rangle$  values and provide information on the role of the size of the non-tetrahedral cations in defining structural "stability." Accordingly, it may be possible to accurately predict the cell edges and oxygen positional parameters for a number of likely  $\{X\}$  and  $[Y]$  cations, calculate the hypothetical garnet structures, and then decide whether the structural data for the given cations are reasonable in terms of certain assumptions. Figure 9 was prepared from an examination of the structural details of over 200 combinations of  $\langle r\{X\} \rangle$  and  $\langle r\{Y\} \rangle$ , respectively, ranging from 0.80 to 1.50 Å and 0.50 to 1.15 Å in increments of 0.05 Å. To establish the structural "stability" of a hypothetical silicate garnet, the following assumptions were made:

1. The mean Si-O bond length cannot be longer than 1.66 Å. (This is 0.02 Å larger than the expected value of 1.64 Å for orthosilicates with 4-coordinated oxygens (Brown and Gibbs, 1969 and Shannon and Pre-

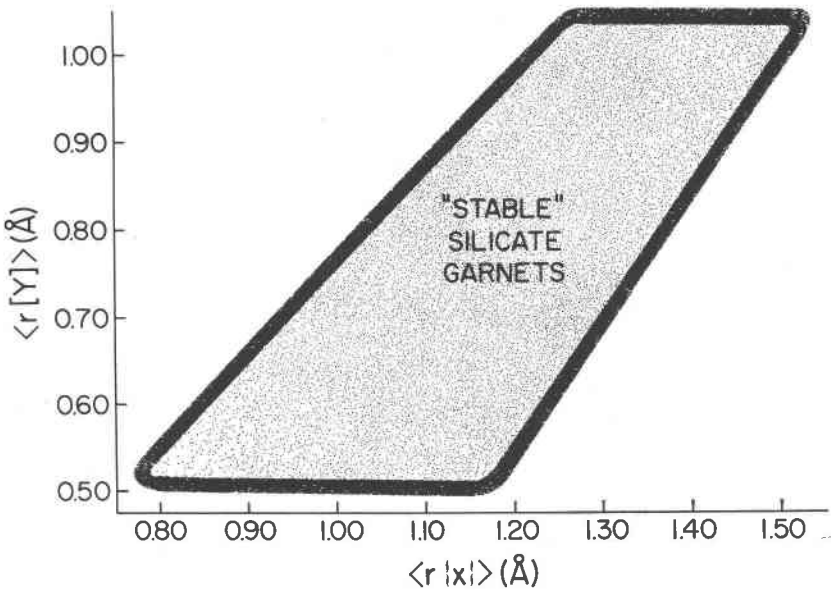


FIG. 9. "Stability" field for silicate garnets prepared from over 200 hypothetical structures predicted solely from  $\langle r\{X\} \rangle$  and  $\langle r[Y] \rangle$ .

witt, 1969) and is 0.005 Å longer than the longest Si-O bond length (goldmanite) found in garnets.)

2. Oxygen-oxygen distances of unshared octahedral edges cannot be less than 2.68 Å. (This assumption may be violated for one or two unshared edges of an octahedron, but in garnet, where the symmetry of the octahedron is high ( $S_6$ ) a violation would result in six short edges with considerable destabilization.)

3. The size of the octahedral cavity should be compatible with the size of the [Y] cation in that the sum of Shannon and Prewitt's radii ( $Y+O$ ) cannot be more than 0.05 Å greater than the predicted  $Y-O$  distance. (Violation of this assumption would place cations in a rigid cavity that is too small. The largest observed difference (0.02 Å) between ( $Y+O$ ) and the  $Y-O$  distance is found for pyrope.)

4. The size of the dodecahedral cavity should be compatible with the size of the {X} cation in that ( $X+O$ ) cannot be more than 0.13 Å greater than the predicted  $\langle X-O \rangle$  distance. (The largest observed difference (0.09 Å) between ( $X+O$ ) and  $X-O$  is found for grossular.)

The structural "stability" field of Figure 9 was determined by applying these four assumptions to hypothetical silicate garnet structures resulting from the more than 200 combinations of  $\langle r\{X\} \rangle$  and  $\langle r[Y] \rangle$ .

The top limit of the field is determined by violations of assumption 1. Structures above this fringe have Si-O bond lengths longer than 1.66Å. The bottom portion is determined from violations of assumption 2. Unless the [Y] cation is sufficiently large to buttress the structure, the unshared octahedral edges become less than 2.68Å, the assumed lower limit. The left limit of the field is determined by violations of assumption 3. For given values of  $\langle r\{X\} \rangle$  and  $\langle r[Y] \rangle$ , structures to the left of the fringe have Y-cavities too small to accommodate the [Y] cation. Finally, the right limit is determined by violations of assumption 4. To the right of this fringe, the {X} cation is too large to fit the dodecahedron.

All known silicate garnets fall within the delineated field. Also, all the compositions enumerated in Table 15, with the exception of the [Y]=Al garnets with {X}=Sr or Ba, can probably be synthesized into stable silicate garnets, if proper oxidation states and experimental conditions can be obtained. The "fringe" of the field designates garnets that may be synthesized, but with difficulty.

Zemann (1962) and Born and Zemann (1964) have indicated that Ca represents the upper limit and Mg the lower limit of the size of the {X} cations for the [Y]=Al garnets. They appear to be correct for {Ca} in that larger cations would produce unshared octahedral edges less than 2.68Å. On the other hand, our study indicates that cations slightly smaller than {Mg} might be stably incorporated in garnet, but only under extreme pressures since the dimensions of the dodecahedra cavities are significantly larger than (X+O). However, if the {X} cation is more than 0.1Å smaller than {Mg} the [Y] cation will be more than 0.05Å larger than its confining cavity.

It must be emphasized that Figure 9 is a "stability" diagram based only on the sizes of the divalent X- and trivalent Y-cations for silicate garnets. It may not be applicable to cations in other oxidation states, nor to non-silicate garnets with smaller (Z) cations (which would have the effect of reducing the minimum and maximum values of  $\langle r\{X\} \rangle$  and  $\langle r[Y] \rangle$ ) or with large (Z) cations (which would have the effect of raising the minimum and maximum values of  $\langle r\{X\} \rangle$  and  $\langle r[Y] \rangle$ ).

In conclusion the structures of the cubic silicate garnets can be rationalized in terms of a hard sphere model in spite of the diverse nature of the substituent non-tetrahedral cations. Even more remarkable is that the cell edges and bond lengths and angles can be predicted for these garnets with a fair degree of accuracy solely in terms of the assumption of additivity of ionic radii. Examination of the predicted structures in terms of certain criteria, such as reasonable Si-O and O-O distances and octahedral and dodecahedral cavities that conform to the sizes of the

[Y] and {X} cations, permits an understanding of the role played by these substituent cations in determining structural "stability." Furthermore, it is possible to establish a "stability" field for the silicate garnets which predicts the sizes of the substituent cations that can be stably incorporated into the structure. All cubic silicate garnets known to exist fall within this field.

## ACKNOWLEDGEMENTS

The authors wish to thank Doctors F. D. Bloss, P. H. Ribbe, and M. W. Phillips of the Department of Geological Sciences, the Virginia Polytechnic Institute and State University at Blacksburg, Virginia and Doctor G. E. Brown of the Department of Earth and Space Sciences, State University of New York, Stony Brook, New York for their many useful suggestions throughout this project and for critically reviewing the manuscript. The National Science Foundation is gratefully acknowledged for supporting grants GA-1133 and GA-12702 at Virginia Polytechnic Institute.

## REFERENCES

- ABRAHAM, S. C., AND S. GELLER, (1957) Refinement of the structure of a grossularite garnet. *Acta Crystallogr.* **11**, 437-441.
- BERTAUT, F., AND F. FORRAT (1956) Structure des ferrites ferrimagnétiques des terres rare. *C. R. Acad. Sci.* [Paris], **243**, 382-384.
- BORN, L., AND J. ZEMANN (1964) Abstrandsberechnungen und gitterenergetische Berechnungen an Granaten. *Contrib. Mineral. Petrology* **10**, 2-23.
- BROWN, G. E. (1970) *The crystal chemistry of the olivines*. Ph.D. Dissertation, Virginia Polytechnic Institute and State University.
- , AND G. V. GIBBS (1969) Oxygen coordination and the Si-O bond. *Amer. Mineral.* **54**, 1528-1539.
- (in press) Stereochemistry and ordering in the tetrahedral portion of silicates. *Amer. Mineral.*
- (in press) The crystal chemistry of the olivines. *Amer. Mineral.*
- BURNHAM, C. W. (1963) Refinement of the crystal structure of kyanite. *Z. Kristallogr.* **118**, 337-360.
- BUSING, W. R., K. O. MARTIN, AND H. A. LEVY (1962) ORFLS, a Fortran crystallographic least-squares refinement program. *U. S. Clearinghouse Fed. Sci. Tech. Info. Doc.*, ORNL-TM-305.
- (1964) ORFFE, a Fortran crystallographic function and error program. *U. S. Clearinghouse Fed. Sci. Info. Doc.*, ORNL-TM-306.
- CHINNER, G. A., AND J. SCHAIRER (1962) The join  $\text{Ca}_3\text{Al}_2\text{Si}_3\text{O}_{12}\text{-Mg}_3\text{Al}_2\text{Si}_3\text{O}_{12}\text{-CaO-MgO-Al}_2\text{O}_3\text{-SiO}_2$  at atmospheric pressure. *Amer. J. Sci.* **260**, 611-634.
- COES, L. (1955) High pressure minerals. *Amer. Ceram. Soc.* **38**, 298.
- CRUICKSHANK, D. W. J. (1965) Errors in least-squares methods. In J. S. Rollett, Ed. *Computing Methods in Crystallography*. Pergamon Press, New York, 112-116.
- DILLON, J. F., JR. (1958) Optical properties of several ferrimagnetic garnets. *J. Appl. Phys.* **29**, 539-541; 1286-1291.
- DOYLE, P. A., AND P. S. TURNER (1968) Relativistic Hartree-Fock x-ray and electron scattering factors. *Acta. Crystallogr.* **A24**, 390-397.
- EULER, FERDINAND, AND JANE A. BRUCE (1965) Oxygen coordinates of compounds with garnet structures. *Acta. Crystallogr.* **19**, 971-978.

- FRONDEL, CLIFFORD, AND JUN ITO (1965) Stilpnomelane and spessartite-grossularite from Franklin, New Jersey. *Amer. Mineral.* **50**, 498-501.
- FYFE, W. S. (1954) The problem of bond type. *Amer. Mineral.* **39**, 991-1004.
- GELLER, S. (1967) Crystal chemistry of the garnets. *Z. Kristallogr.* **125**, 1-47.
- , AND M. A. GILLES (1957) Structure and ferrimagnetism of yttrium and rare earth iron garnets. *Acta Crystallogr.* **10**, 239.
- GELLER, S., AND C. E. MILLER (1959a) The synthesis of uvarovite. *Amer. Mineral.* **44**, 445-446.
- , AND ——— (1959b) Silicate garnet-yttrium iron garnet solid solutions. *Amer. Mineral.* **44**, 1115-1120.
- GELLER, S., AND C. E. MILLER (1959c) Substitution of  $\text{Fe}^{2+}$  for  $\text{Al}^{3+}$  in synthetic spessartite. *Amer. Mineral.* **44**, 665-667.
- , AND R. G. TREUTING (1960) New synthetic garnets. *Acta Crystallogr.* **13**, 179-186.
- GELLER, S., H. J. WILLIAM, G. P. ESPINOSA, AND R. C. SHERWOOD (1964) Importance of intrasublattice magnetic interactions and of substitutional ion type in the behavior of substituted yttrium iron garnets. *Bell System Tech. J.* **43**, 565-623.
- GENTILE, A. L., AND R. ROY (1960) Isomorphism and crystalline solubility in the garnet family. *Amer. Mineral.* **45**, 701-711.
- GEUSIC, J. E., H. M. MARCOS, AND L. G. VAN UITERT (1964) Laser oscillations in Nd-doped yttrium aluminum, yttrium gallium and gadolinium garnets. *Appl. Phys. Lett.* **4**, 182-184.
- GIBBS, G. V., AND J. V. SMITH (1965) Refinement of the crystal structure of synthetic pyrope. *Amer. Mineral.* **50**, 2023-2039.
- GRIFFITH, W. P. (1969) Raman studies on rock-forming minerals—Part 1. Orthosilicates and cyclosilicates. *J. Chem. Soc. A*, 1372-1377.
- HAMILTON, W. C. (1965) Significance tests on crystallographic R-factors. *Acta Crystallogr.* **18**, 502-510.
- HANSON, A. W. (1965) The crystal structure of the azulene, S-tri-nitrobenzene complex. *Acta Crystallogr.* **19**, 19-26.
- HOARD, J. L., AND J. V. SILVERTON (1963) Stereochemistry of discrete eight-coordination. I. Basic analysis. *Inorg. Chem.* **2**, 235-243.
- Hsu, L. C. (1968) Selected phase relations in the system Al-Mn-Fe-Si-O-H: A model for garnet equilibria. *J. Petrology* **9**, 30-46.
- , AND C. W. BURNHAM (1969) Phase relationships in the system  $\text{Fe}_3\text{Al}_2\text{Si}_3\text{O}_{12}$ - $\text{Mg}_3\text{Al}_2\text{Si}_3\text{O}_{12}$ - $\text{H}_2\text{O}$  at 2.0 kilobars. *Geol. Soc. Amer. Bull.* **80**, 2393-2408.
- HUCKENHOLZ, H. G. (1969) Synthesis and stability of Ti-andradite. *Amer. J. Sci., Shairer Vol.* **267A**, 209-232.
- ITO, JUN, AND CLIFFORD FRONDEL (1968) Synthesis of the grossularite-spessartite series. *Amer. Mineral.* **53**, 1036-1038.
- KIMBALL, G. E. (1940) Directed valencies, *J. Chem. Phys.* **8**, 188.
- KOHN, J. A., AND D. W. ECKART (1962) X-ray study of synthetic diamond and associated phases. *Amer. Mineral.* **47**, 1422-1430.
- LIND, M. D., AND S. GELLER (1969) Crystal structure of the garnet  $\{\text{Mn}_3\}\{\text{Fe}_2\}(\text{Ge}_3)\text{O}_{12}$ . *Z. Kristallogr.* **129**, 427-433.
- LIPPARD, S. J., AND B. J. RUSS (1968) Comment on the choice of an eight-coordination polyhedron. *Inorg. Chem.* **9**, 1686-1688.
- McCONNELL, D. (1964) Refringence of garnets and hydrogarnets. *Can. Mineral.* **8**, 11-22.
- (1966) Propriétés physiques des grenates. Calcul de la dimension de la maille unité à partir de la composition chimique. *Bull. Soc. Franc. Minéral. Cristallogr.* **89**, 14-17.
- MENZER, G. (1926) Die Kristallstruktur von Granat. *Z. Kristallogr.* **63**, 157-158.
- (1928) Die Kristallstruktur der Granate. *Z. Kristallogr.* **69**, 300-396.

- MILL', B. V. (1964) Hydrothermal synthesis of garnets containing  $V^{3+}$ ,  $In^{3+}$  and  $Sc^{3+}$ . *Dokl. Akad. Nauk. USSR* **156**, 814–816.
- (1966) Hydrothermal synthesis of silicates and germanates with garnet structure type *Zhur. Neorg. Khim.* **11** 1533–1538 [in Russian].
- MOENCH, ROBERT H., AND ROBERT MEYROWITZ (1964) Goldmanite, a vanadium garnet from Laguna, New Mexico. *Amer. Mineral.* **49**, 644–655.
- MOORE, R. K., W. B. WHITE, AND T. V. LONG (1969) Vibrational spectra of silicate garnets. [abstr.], *Trans. Amer. Geophys. Union* **50**, 358.
- NĚMEC, D. (1967) The miscibility of the pyralspite and grandite molecules in garnets. *Mineral. Mag.* **37**, 389–402.
- NOVAK, GARY A., AND HENRY O. A. MEYER (1970) Refinement of the crystal structure of a chrome pyrope garnet: An inclusion in natural diamond. *Amer. Mineral.* **55**, 2124–2127.
- NOVAK, GARY A., AND HENRY O. A. MEYER (in press) Refinement of the crystal structure of a chrome pyrope garnet: An inclusion in natural diamond. *Amer. Mineral.*
- PAULING, L. (1929) The principles determining the structure of complex ionic crystals. *J. Amer. Chem. Soc.* **51**, 1010–1026.
- PRANDL, WOLFRAM (1966) Verfeinerung der Kristallstruktur des Grossulars mit Neutronen und Röntgenstrahlbeugung. *Z. Kristallogr.* **123**, 81–116.
- PREWITT, C. T., AND A. W. SLEIGHT (1969) Garnet-like structures of high-pressure cadmium germanate and calcium germanate. *Science* **163**, 386–387.
- QUARENI, S., AND R. DE PIERI (1966) La struttura Dell' andradite. *Mem. Accad. Patavina, Sci. Mat. Nat.* **78**, 153–164.
- RICKWOOD, P. C. (1968) On recasting analyses of garnet into end-members. *Contrib. Mineral. Petrology* **18**, 175–198.
- ROBINSON, K., G. V. GIBBS, AND P. H. RIBBE (In press) Quadratic elongation: A quantitative measure of distortion in coordination polyhedra. *Science*
- RUCKLIDGE, JOHN, AND E. L. GASPARRINI (1968) *EMPADR V*. Department of Geology, University of Toronto.
- SHANNON, R. D., AND C. T. PREWITT (1969) Effective ionic radii in oxides and fluorides. *Acta Crystallogr.* **B25**, 925–946.
- SKINNER, B. J. (1956) Physical properties of end-members of the garnet group. *Amer. Mineral.* **41**, 428–436.
- SMITH, J. V. (1965) X-ray-emission microanalysis of rock-forming minerals. I. Experimental techniques. *J. Geol.* **73**, 830–864.
- STRENS, R. G. (1965) Synthesis and properties of calcium vanadium garnet (goldmanite). *Amer. Mineral.* **50**, 260.
- SWANSON, H. E., M. I. COOK, E. H. EVANS, AND J. H. DE GROOT (1960) Standard x-ray diffraction powder patterns. *Nat. Bur. Stand. [U.S.] Circ.* **539**, no. 10, 17–18.
- , T. ISAACS, AND E. H. EVANS (1960b) Standard x-ray diffraction powder patterns. *Nat. Bur. Stand. [U.S.] Circ.* **539**, no. 9, p. 22–23.
- WINCHELL, A. N. (1933) *Optical Mineralogy II*, 3rd ed., New York, John Wiley and Sons, Inc.
- YODER, H. S., JR. (1950) Stability relations of grossularite: *J. Geol.* **58**, 221–253.
- YODER, H. S., JR., AND M. L. KEITH (1951) Complete substitution of aluminum for silicon: The system  $3MnO \cdot 3SiO_2 - 3Y_2O_3 \cdot 5Al_2O_3$ . *Amer. Mineral.* **36**, 519–533.
- ZEMANN, A., AND J. ZEMANN (1961) Verfeinerung der Kristallstruktur von Synthetischem Pyrope,  $Mg_3Al_2(SiO_4)_2$ . *Acta Crystallogr.* **14**, 835–837.
- ZEMANN, J. (1962) Zur Kristallchemie der Granate. *Beitr. Mineral. Petrology* **8**, 180–188.